MEMBRANE FILTRATION OF MICROPLASTIC FIBERS

MEMBRANE FILTRATION OF MICROPLASTIC FIBERS: ASSESSMENT OF MEMBRANE, MICROPLASTIC, AND SOLUTION PROPERTIES

By

Blake Patterson, B. Eng. Society

McMaster University

Department of Chemical Engineering

A thesis submitted to the School of Graduate Studies in partial fulfillment of the requirements of McMaster University for the degree of Master of Applied Science

McMaster University

Master of Applied Science (2021) McMaster University

(Chemical Engineering) Hamilton, Ontario

Title: MEMBRANE FILTRATION OF MICROPLASTIC FIBERS: ASSESSMENT OF MEMBRANE, MICROPLASTIC, AND SOLUTION PROPERTIES

Author: Blake Patterson

Supervisors: Dr. David Latulippe

Dr. Todd Hoare

Number of Pages: xiii, 80

Lay Abstract

Microplastics, plastic particles that are less than 5 mm in size, have been found throughout the environment due to increasing plastic production and use. Microplastics pose a significant threat to aquatic life as when ingested, microplastics can have negative impacts on the development, behaviour, and mortality of aquatic organisms. Wastewater treatment plants have been found to be a significant source through which microplastics enter the environment as microbeads from personal care products and microplastic fibers from the laundering of synthetic textiles are discharged into municipal sewage systems. Membrane filtration systems used in some wastewater treatment plants have been shown to be effective for microplastic removal but few studies exist examining the filtration of microplastics in depth. In this work, microplastic fibers were manufactured, mimicking those found in wastewater treatment plants, to use in membrane filtration experiments. The impact of membrane properties, solution chemistries, and microplastic fiber properties on membrane filtration were examined.

Abstract

Microplastics (MPs), plastic particles less than 5 mm in size, have become ubiquitous in the environment due to increasing plastic production and pollution. MPs pose a significant threat to both aquatic life and human health due to their small size and heterogeneity in shape (e.g. fragments, fibers, films etc.) and chemistry (e.g. polyethylene, polystyrene, polypropylene etc.) A significant source from which MPs can enter the environment is the effluents of wastewater treatment plants (WWTPs). Membrane filtration systems, used in some WWTPs, have been shown to be effective at removing MPs, as most MPs are larger than the membrane pores. Understanding the impacts MPs have on membrane filtration is a growing area of interest due to their potential adverse effects, though all studies to date have been focused specifically on MP fragments. As MP fibers (MPFs) are common in both the influents and effluents of membrane systems in WWTPs, it is important to understand their impact on membranes and how they can be removed. In this work, polystyrene was electrospun into a fiber mat, which was cut using a cryostat to yield MPFs. Fluorescent MPFs were created by doping the electrospinning solution with meso-tetraphenylporphyrin, enabling the detection of MPFs in suspension. These MPFs were used to investigate the impacts of membrane pore size, solution chemistry, and MPF length on the removal of MPFs and membrane fouling. MPFs were found in the permeate of a 5 μm membrane, with some MPFs exceeding the nominal membrane pore size. Feed suspensions with shorter MPFs were found to result in more MPFs passing through the membranes compared to feed suspensions with wider variation in MPF lengths. When MPFs were suspended in real WW, both 0.22 μm and 5 μm membranes experienced more fouling compared to when MPFs were suspended in Milli-Q water. This work highlights the importance of working with solutions and particles realistic to those found in WWTPs and the environment to better understand the impact MPFs can have on membrane filtration.

Acknowledgements

First, I would like to thank my supervisors Dr. David Latulippe and Dr. Todd Hoare for their continuous guidance, support, and encouragement. Your insight and supervision has been invaluable. Thank Dr. David Latulippe for seeing my potential and allowing me to starting working in your lab during undergrad, which ignited my interest in research. I would also like to thank Dr. Jose Moran-Mirabal for being part of my committee and providing your expertise and advice. I would like to thank Dr. Jake Nease for letting me be a teaching assistant for Chem Eng 2E04 and inspiring my interest in teaching.

I would like to acknowledge the help of Marta Prince and Mehdi Keramane in the Biointerfaces Institute for training and assistance in using their equipment, which made this work possible. As well, I would like to thank the Canadian Center for Electron Microscopy and specifically Jhoynner Martinez training and support when using the SEM. I would also like to thank Mary Jo Wilson from the McMaster Histology Facility for her training and guidance in using the cryostat instrument. Also, thank you to the Dundas Wastewater Treatment Plant for supplying the secondary clarifier water used for filtration experiments.

Financial support for my research was provided by the Natural Sciences and Engineering Research Council of Canada (NSERC) through the Canadian Graduate Scholarship – Master's program and by the Province of Ontario through the Ontario Graduate Scholarship.

I would like to thank the members of both the Latulippe and Hoare labs. It was great getting to know and working with you during our studies. I would like to thank Amir, Ryan, and Michael for being great mentors and inspiring my interest in research. I would also like to acknowledge the undergraduate students who have worked on projects related to microplastics, Brianna and

Ashleigh. You both have bright futures ahead of you and I wish you luck in all of your future endeavours.

Lastly, I would like to thank my friends and family who have been a huge support throughout my education. Thank you to Paulina, Jaime, Asia, Rosa, Beckie, and Victoria for the encouragement, game nights, and walks that helped keep me sane. Jaime, I'm excited to graduate with you for the fourth time. Thank you to both my parents for their support and constant encouragement throughout my academic career. Thank you to my mom Fran for your continuous support and patience as well as the many phone calls and visits. Thank you to my dad Kevin for believing in me and encouraging me to pursue my education. Finally, thank you to my partner Daniel for your unconditional support and encouragement throughout this whole process. Thank you for always believing in me, even when I didn't.

Table of Contents

List of Figures

List of Tables

Abbreviations & Symbols

c20 MPFs	Microplastic Fibers cut at 20 µm
c100 MPFs	Microplastic Fibers cut at 100 µm
COD	Chemical Oxygen Demand
DMF	Dimethylformamide
HF	Hollow fiber
J	Flux
L_{av}	Average Length
LMH	$L/m^2/h$ (units of flux)
Lp	Hydraulic Permeability
Lp0	Initial Hydraulic Permeability
Lpf	Final Hydraulic Permeability
MBR	Membrane Bioreactor
MF	Microfiltration
MP	Microplastic
MPF	Microplastic Fiber
MQ	Milli-Q Water
N	Number of Microplastic Fibers
NF	Nanofiltration
NP	Nanoplastic
PC	Polycarbonate
PES	Polyether Sulfone
PS	Polystyrene
PVC	Polyvinyl Chloride
PVDF	Polyvinylidene Fluoride
RO	Reverse Osmosis
RPM	Rotations Per Minute
SEM	Scanning Electron Microscopy
TC	Total Carbon
TOC	Total Organic Carbon
TMP	Transmembrane Pressure
TPP	Tetraphenylporphyrin
TS	Total Solids
UF	Ultrafiltration
WW	Wastewater
WWTP	Wastewater Treatment Plant

Declaration of Academic Achievement

This work has been written in the format outlined below. Some information in the introduction and methods is the same between chapters but all results presented are unique

- Chapter 2: B. Patterson, R.J. LaRue, A. Warren, T. Hoare, D. R. Latulippe, Assessment of solution and membrane properties on microplastic fiber filtration.
- Chapter 3: B. Patterson, Understanding the impact of fiber length on membrane filtration using fluorescent microplastic fibers.

The content in Chapter 2 has been reproduced from a prepared manuscript intended for publication. Blake Patterson is responsible for the planning, performing, analyzing, and writing of the content presented in all chapters between May 2019 – July 2021. Dr. David Latulippe and Dr. Todd Hoare have co-supervised the completion of this work contributing to planning, writing, and revising the chapters over the same time period. Ashleigh Warren, under the mentorship of Ryan LaRue, completed a literature review of studies investigating membrane filtration of microplastics within wastewater treatment plants in summer 2020, some of the results from which are included in Chapter 1 and the introduction to Chapter 2.

Chapter 1: Introduction

1.1 Classification and Origin of Microplastics

Plastics have become a significant part of everyday life, with world plastic production reaching 359 million metric tonnes in 2018 [1]. Plastics have significant societal benefits but their increased use and rapid disposal has led to serious consequences. A significant negative impact of the increasing use and production of plastic items is microplastics (MPs), which are small plastic particles. MPs can vary from 1 µm to 5 mm in size [2][3]. Plastic particles smaller than 1 µm are often referred to as nanoplastics (NPs), though the characterization of NPs has not formally been recognized as they are difficult to detect in water and soil samples [4] [5]. There is also no standard technique for the detection of MPs which allows for significant variation in the sizes of MPs collected between studies. MPs can have a wide variety of properties specifically in terms of size, shape, and chemistry. As shown in Figure 1.1, MPs are often characterized in terms of their shape such as fragments, fibers, films, foams, granules, and microbeads [6]. MP shape is often determined by the original source of the particle, which can be from a primary or secondary source. Primary MPs are plastic particles that were specifically manufactured to be less than 5 mm in size; for instance microbeads found in many personal care products [7]. Secondary MPs are created from the physical and/or chemical degradation of larger plastic items; for instance, clothing made of synthetic materials such as polyester or nylon has been shown to produce large amounts of MP fibers (MPFs) in the discharged water from laundry machines [8]. Plastic items can also degrade due to photo-oxidation, high temperatures, and abrasion when disposed [7][9].

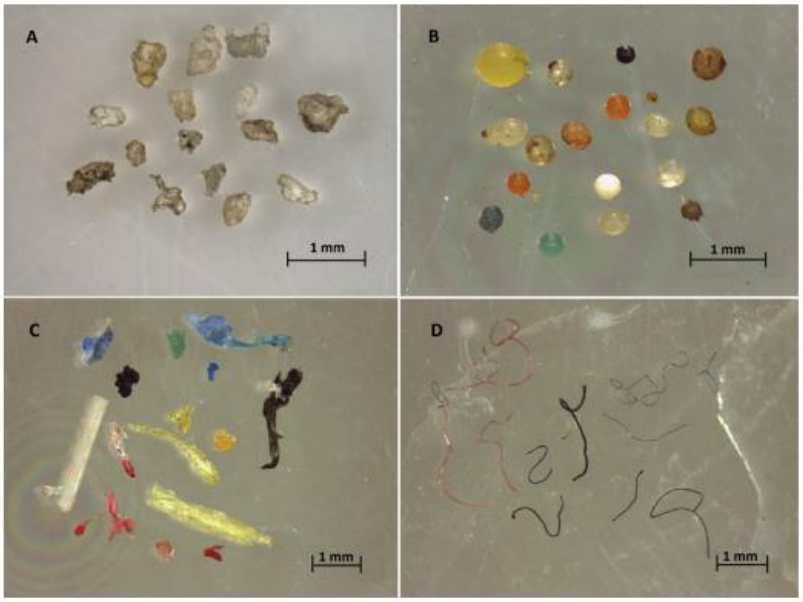

Figure 1.1. MPs of different shapes; (A) fragments, (B) microbeads, (C) films, (D) fibers. Adapted from [10].

MPs are also commonly classified based on their chemistry; the most prevalent ones found in water and sediment samples being polyethylene, polypropylene, polystyrene, polyamide, polyester, and acrylic [10]. However, the addition of various additives such as plasticizers, stabilizers, and colourants to certain plastic products makes the composition more complex [9]. It has been shown that certain additives can leach out of MPs due to their instability within plastic products [7]. MP chemistry and shape are somewhat correlated - for instance MPFs are often polyester, polyamide, and acrylic as they are generated by the laundering of clothing made from synthetic materials whereas MP fragments are often reported being made of polyethylene and polypropylene [10].

1.2 Impacts of Microplastics on the Environment and Human Health

MPs have been found in marine environments [2], freshwater ecosystems [11], and sediments [12] across the world, being identified on coastlines in all continents as well as major

freshwater lakes [13]. In one of the first studies of its kind, Eriksen et al [14] sampled 21 sites across three of the Great Lakes (Lake Superior, Lake Huron, and Lake Erie) and found an average MP concentration of 43,000 MPs/km^2 across all sites, with sites located near major cities having MP concentrations of up to 466,000 MPs/km^2. MP transport can also occur through the atmosphere, over distances up to 95 km, allowing MPs to reach remote areas with minimal inhabitants [15]. MPs are a threat to aquatic organisms in multiple ways. The ingestion of MPs that are similar size to their food sources by aquatic organisms can have a variety of negative impacts including decreased reproductive output [16], impaired feeding [17], and reduced energy available for growth [18][16]. MPs have the potential to cause internal blockages within organisms. MPFs have been found to get stuck in the respiratory system of aquatic organisms [19] as well as the stomach, intestines, and gills of fish [20]. MPs have been shown to have an inherent toxicity to wildlife via leaching of chemicals added during the plastic manufacturing process, and/or the adsorbed contaminants from the environmental matrix in which the MPs are present [11][21][7]. For example, Teuten et al [22]found that polychlorinated biphenyls transferred from contaminated plastic particles to streaked shearwater chicks when the plastic particles were ingested. The presence of MPs has been found to increase the uptake of contaminants, leading to increases in mortality and acute toxic effects [23].

MP size can have a significant impact on ingestion and retention when ingested. NPs have been found to be more easily ingested by aquatic organisms and have slower excretion compared to larger MPs [24], leading to an increase in retention time [25][26]. As well, the toxicity of MPs can be size dependent, with smaller MPs being more toxic [25]. NPs have been specifically associated with accumulation in organisms such as algae, planktonic crustaceans, mussels, oysters, fish, sea urchins, shrimp, and rodents, with a potential to cause decreased survival rate,

developmental defects, and altered behaviour [4]. NPs are also able to be transported through the body in fish more easily than larger MPs, reaching the nervous system and brain [27]. Though small aquatic organisms at lower trophic levels are more likely to be contaminated by MP pollution, ingesting MPs can lead to MPs transferring through the food web to larger organisms [28][29]. Larger predatory fish may ingest MPs due to their own feeding habits or by ingesting prey that have ingested MPs [30]. Mattsson et al [31] found that polystyrene NPs transferred from algae to zooplankton to fish, where they reduced the survival of zooplankton and caused behavioral disorders in fish. MPs have been found inside of fish that are caught for human consumption [30]. MP ingestion has been studied for 7 out of the 10 most farmed aquaculture species, where the average amount of MPs per organism was found to be 1.9 -3.8 MPs/individual [29]. For studies that investigated MP properties as well as ingestion, MPFs made up 57.6-86.5% of MPs observed [29]. Of the 10 most caught marine fish, the percentage of organisms with MPs found in their gastrointestinal tract ranges from 0.9 – 76.6% [29]. MPFs were also the most common MP shape observed, making up 30-87.6% of MPs [29]. The increased risks associated with smaller MPs in the environment is also cause for concern due to the lack of standardized MP detection methods as well as the degradation of larger MPs. Current methods for MP characterization and detection are not able to accurately isolate or quantify NPs and as a result the fate of smaller MPs in the environment is largely unknown [4].

With the increase in MPs found in the environment, there has been growing attention in how MPs may impact humans. Humans have been found to be at higher risk of MP ingestion when consuming smaller fish, shellfish, and edible seaweeds than when ingesting larger fish as often the gastrointestinal tract, where MPs tend to collect, is removed before consumption [29]. Shellfish consumers are estimated to ingest 4620 - 11,000 MPs per year [32][33]. MPs have been found in

drinking water sources, including bottled water, with concentrations ranging from 0.0007 to 6292 MPs/L [9]. Mason et al [34] found that out of 259 bottled water samples processed, 93% were found to contain MPs. Humans can also be exposed to MPs via beverages such as soft drinks, energy drinks, cold teas, and beer in concentrations from 0-28MPs/L, with MPs originating from synthetic textiles and beverage packaging [35]. Synthetic tea bags used for hot tea can degrade when steeped resulting in the release of billons of MPs and NPs [36].

Humans also can ingest MPs from those that are airborne. Fibers are present in indoor dust, 33% being made of synthetic polymers [37]. While having a meal, a person can be exposed to 13,371 – 68,415 airborne fibers per year [33]. Though MPFs found in waters and sediments are often too large for humans to ingest, those found in dust have the potential to be inhaled [37]. Most MPFs are likely cleared naturally by the respiratory system, MPFs that remain in the lungs can cause an inflammatory response [38]. Ingestion of MPs can result in the exposure to contaminants associated with MPs, similar to aquatic organisms. This exposure has the potential to cause effects as low doses of plasticizers and additives used in the plastic manufacturing process have been found to cause endocrine disruption in humans [39]. Despite these risks, MPs are unlikely to cause human health impacts but the effects of long term exposure to MPs through ingestion or inhalation are largely unknown [40].

1.3 Sources of Microplastics

A significant source of MPs into aquatic environments are the effluent streams from wastewater treatment plants (WWTPs) [41]. Primary and Preliminary treatment technologies in WWTPs including sedimentation tanks and solids skimming are effective at removing up to 50% of MPs 100 – 5000 µm in size and over 99% of MPs are removed after secondary treatment (e.g.

bioreactor, secondary sedimentation/filtration) [42][43][44]. Though primary and secondary treatment steps are able to remove majority of larger MPs, smaller MPs are still found in the effluent which gets discharged into our lakes and rivers [44]. A study by Mintenig et al [45] investigating 12 WWTPs with daily effluxes between 500 – 35,000 m^3 found that an individual WWTP can release up to 10^{10} MPs per day. As well, the unit operations in WWTPs can cause fragmentation of MPs, resulting in the formation of smaller MPs which are more difficult to remove [46]. Often smaller MPs are not accounted for when samples of WW or WWTP sludge are examined due to the choice of sampling, purification, and quantification methods which often don't allow for the detection of MPs smaller than 1 µm [46][47]. Through an analysis of 76 studies, Koutnik et al [47] found that 96% of MPs removed in WWTPs are unaccounted for. The removal of MPs from the treated water results in these MPs being contained in the sludge from WWTPs which can be transported to landfill or used as fertilizer on agricultural soils [43][48]. Sludge disposal can also lead to the release of MPs into aquatic environments as MPs can enter the leachate from landfills or agricultural runoff [49][50].

MPs can enter WWTPs through several avenues. A major source of MPFs is the laundering of synthetic clothing as the water used for washing can contain 640,000 – 1,500,000 MPFs per kilogram of clothing washed [51][52]. The majority of these MPFs are 360 – 660 µm in length and 12 – 16 µm in diameter [51]. Personal care products that contain microbeads such as exfoliants and toothpastes are a source of MPs into WWTP influents with 4594 – 94,500 microbeads 164 – 327 µm in diameter released in a single use [53]. As humans ingest MPs from their food, beverages, and environment, MPs have been found to be present in human stool in concentrations ranging from 1 – 36 MPs/g, ranging from 20 – 800 µm in size, which would also contribute to MPs entering into WWTPs [54].

Though WWTPs are a major source of MPs into aquatic ecosystems, there are several other major routes through which they can pollute the environment. As MPs can originate from the degradation of larger plastic items, MPs can enter aquatic environments through mismanaged plastic waste [55][56]. In 2010, approximately 1.7 – 4.6% of total plastic waste from coastal countries ended up in the ocean, which is estimated to be 4.8 – 12.7 million metric tonnes [55]. Through the degradation pathways described previously, this plastic waste can generate MPs. Even when plastic waste is not mismanaged, it can still create MPs. MPs have been detected in the leachate from landfills with concentrations ranging from 0.42 – 24.58 MPs/L [49]. Over 99% of the MPs detected in leachate were generated by the degradation of larger plastic items within landfills [49]. MPs have been found in higher concentrations surrounding costal landfills as compared to WWTPs [57]. Plastic resin pellets can also be lost during transportation or in areas close to processing plants, resulting in the discharge of MP pellets [5].

1.4 Role of Membrane Technologies in Wastewater Treatment Plants

Membrane systems have become more common to be used for separation and purification due to their high selectivity, continuous operation, and easy scale up. They have been found to be well suited to WW and drinking water treatment due to their ability to recycle and reuse water [58]. Membranes are barriers which can selectively separate two phases and restrict transport of components based on size, charge, or shape [59][60]. Membranes that separate based on size are often categorized based on their nominal pore size, which gives an indication of the size range of particles they are able to retain. These membranes are classified as microfiltration (MF), ultrafiltration (UF), nanofiltration (NF), and reverse osmosis (RO), pore size ranges for which are shown in Figure 1.2 [60]. The driving force for transport across these membrane types is often the pressure difference between the feed and permeate side of the membrane [60]. With decreasing

pore size, membranes become more selective towards smaller solutes such as ions and salts. This also results in a higher pressure difference across the membrane and lower permeability, demanding higher energy consumption [60].

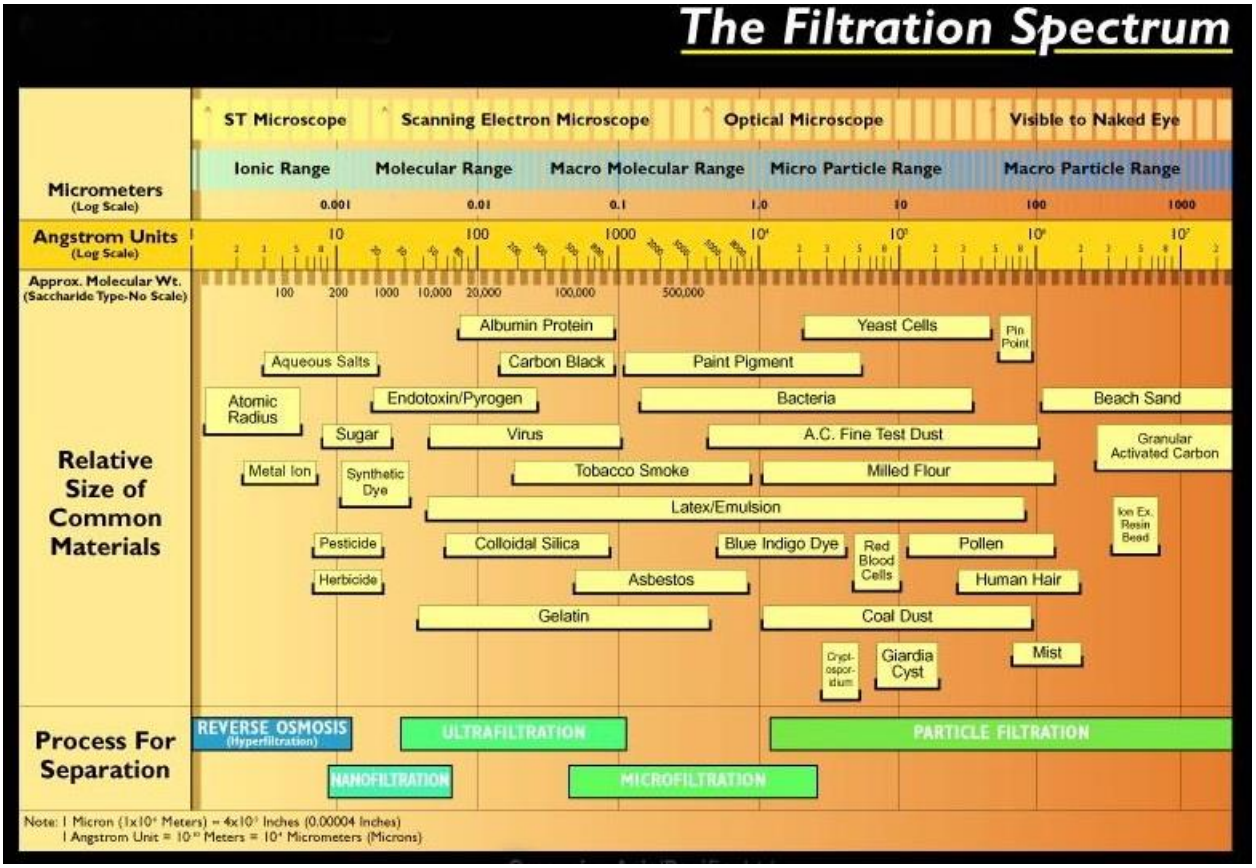

Figure 1.2. Pore sizes ranges for different types of separation processes and size ranges of common contaminants. Adapted from [63].

Membranes for WW or drinking water treatment can be classified by material as well as configuration. Membranes used in pressure driven systems are typically made of organic polymers such as poly(vinylidene fluoride) (PVDF), poly(ether sulfone) (PES), polycarbonate (PC), and cellulose acetate [60]. Ceramic membranes can be used in cases where better thermal, chemical, and mechanical stability is necessary for MF and UF processes [60]. In terms of configuration,

polymeric membranes can be used in plate and frame, tubular, spiral wound, or hollow fiber modules [61]. Spiral wound configurations, where membranes are wrapped around a perforated tube for permeate collection with feed spacers in between layers, are most commonly used for NF and RO processes [61]. Hollow fiber modules, consisting of bundles of small membrane tubes that can be operated in inside-out (feed enters inside of the membrane and permeate exits radially) or outside-in (feed enters from outside of the membrane and permeate travels through the inside of the membrane), are commonly used for UF and MF systems [61]. Both spiral wound and hollow fiber modules allow for high packing density of the membranes, resulting in higher surface area [61]. Both of these types of configurations employ cross-flow filtration, where the feed flow is tangential to the membrane as opposed to dead-end filtration where the feed flow is normal to the membrane surface.

Membrane systems have been used as a tertiary treatment step for polishing WW as the need for water reuse and WWTP effluent standards have increased [62]. Membranes used for this application are commonly hollow fiber modules using UF or MF membranes [62]. A MF or UF module may be followed by an RO system when high effluent water quality is required [62]. Water entering tertiary membranes is often screened to remove larger particles or a coagulant is used. MF systems have been able to remove an average of 97% of turbidity and 47% of COD, with higher removal reducing fouling of the RO system [62]. Despite the difference in pore size, similar water quality has been obtained when comparing MF and UF systems for tertiary treatment, with MF providing some operational advantages including reduced energy consumption and cleaning frequency [63].

Within municipal WWTPs, membranes can be used in combination with an activated sludge process in the form of a membrane bioreactor (MBR) for solid-liquid separation [59]. These

systems are used in substitution of a bioreactor followed by a secondary clarifier as they are able to better retain bioreactor solids [59]. Due to their high effluent quality, small footprint, and lower sludge production, MBRs are seen increasingly in WWTPs. MBRs have two main configurations, external/side-stream, where the membrane module is outside of the bioreactor, or submerged/immersed, where the membrane module is submerged inside of the bioreactor [64]. MBRs typically employ UF or MF membranes to remove suspended solids and flocced bacteria [65]. The membranes used can be hollow fiber, plate and frame, or tubular in configuration [65]. MBRs are prone to fouling, which is the deposition of solids on the membrane surface reducing permeate flux during filtration, which incurs higher maintenance and operating costs [66][65].

1.5 Prior work on Membrane-based Removal of Microplastics

Membrane systems have been noted as a promising technology for the removal of MPs from WWTP effluents due to the small size of membrane pores (0.002 – 10 µm) as compared to the size of most MPs (1 – 5000 µm). To date, there have been two types of studies investigating the filtration of MPs using membranes; full scale studies looking at the filtration of real MPs in WWTPs or pilot plants and laboratory scale studies looking at MP filtration using small scale membrane systems and sourced or manufactured MPs. Full scale studies provide details on MP removal in realistic conditions and give insights into how membrane technologies are able to perform in the presence of MPs. However, due to their complex and highly variable conditions, they are not able to provide significant detail on the interactions between MPs and the membrane. Laboratory scale studies are able to provide more insight on how membrane properties, MP characteristics, and operating parameters impact membrane fouling and MP rejection. This is an emerging area of research, all works being published within the last 5 years, and still has significant knowledge gaps. The following sections describe the findings from both full scale and laboratory scale studies of MP filtration.

1.5.1 Full Scale Studies of Filtration of Microplastics

To date, there have been studies investigating the filtration of MPs using different types of membrane systems in full scale and pilot scale WWTPs. A literature review was conducted focusing on studies involving the removal of MPs in WWTPs using membranes. An analysis of 14 articles was conducted focusing on how membrane and MP properties impact MP removal. Due to the small number of studies in this field as well as variability between studies, and lack of reporting of key parameters, limited conclusions could be drawn. 11 out of 14 of studies investigated the use of MBRs for MP removal. Studies comparing MBRs to other treatment steps such as disc filters, rapid sand filtration, dissolved air filtration, and oxidation ditch have found MBRs to be just as or more effective [67][68][69][70][71].

Of the 12 studies that reported MP concentration, 9 had MP removal efficiencies above 80%, as shown in Figure 1.3. Influent concentrations ranged from 0.28 MP/L to 1444 MP/L [72][73]. There was significant variation in results between studies due to variations in membrane processes, influent conditions, and MP properties, but there was also variation in results between studies with similar processes. For instance, a ceramic MBR with a nominal pore size of 0.2 µm studied by Michielssen et al [74] had a MP removal efficiency of 99.2% for an influent concentration of 60 MP/L. For a similar influent concentration of 68 MP/L, Leslie et al [75] found a MBR with a nominal pore size of 0.08 µm had a removal efficiency of 25%. The variation in results as well as limited information reported does not allow for definite conclusions to be draw between studies. Often MPs larger than the nominal pore size of the membrane used are found in the effluent. Talvitie et al [67] found that an MBR with a 0.4 µm pore size membrane has a removal efficiency of 99.9% and found that the smallest size fraction of MPs (20 – 100 µm) was the most abundant in the permeate. Baresel et al [76][77] had a similar finding for two studies involving a

MBR with a 0.2 µm pore size, finding that MPs larger than 20 µm were not present in the MBR effluent. Ziajahromi et al [72] reported MPs 20 – 190 µm in size in the permeate of tertiary treatment step using an RO membrane despite RO membranes having pore sizes less than 0.5 nm.

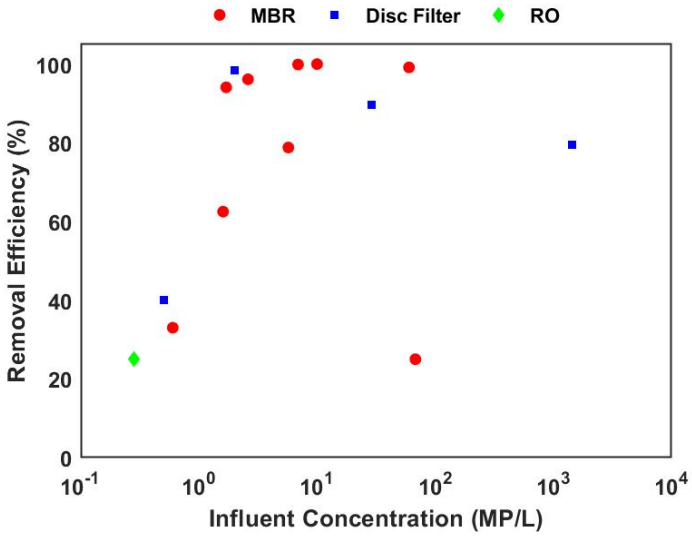

Figure 1.3. MP removal efficiency as a function of influent concentration for studies investigating MP removal using membrane systems.

As shown in Figure 1.4, MPFs make up a significant portion of MPs in the influent and effluent. This figure shows only shape distributions for articles reporting information on MP shape with respect to concentration for both influent and effluent samples. Of the 6 articles providing this information, 5 found that the percentage of MPFs in the effluent was higher than the influent, indicating MPFs are more difficult to remove using membranes. All of the articles quantified MP shape by visually analyzing the MPs under a microscope. Of the articles that also reported MP chemistry, majority of MPFs analyzed were made of polyethylene terephthalate [71][78][72]. Foglia et al [70] reported that all MPs found in the permeate of a hollow fiber MBR with a nominal pore size of 0.03 µm were MPFs. Michielssen et al [74] had a similar finding, reporting that 80% of MPs in the effluent of a MBR using a 0.2 µm ceramic disc membrane were MPFs. Lares et al [78] found that MPFs were the dominant shape found in samples throughout the WWTP studied,

making up more than 50% of each sample. MPFs have been found to have lower removal efficiencies than MP fragments. Bayo et al [68] found that MPFs had a removal efficiency of 57.65% compared to MP particles having a 98.83% removal efficiency for a MBR. Despite high overall MP removal, shape properties can be a determining factor in MP rejection. MPFs may be able to pass through membrane pores longitudinally, especially under high pressure, being able to fit into membrane pores due to their small diameter [75].

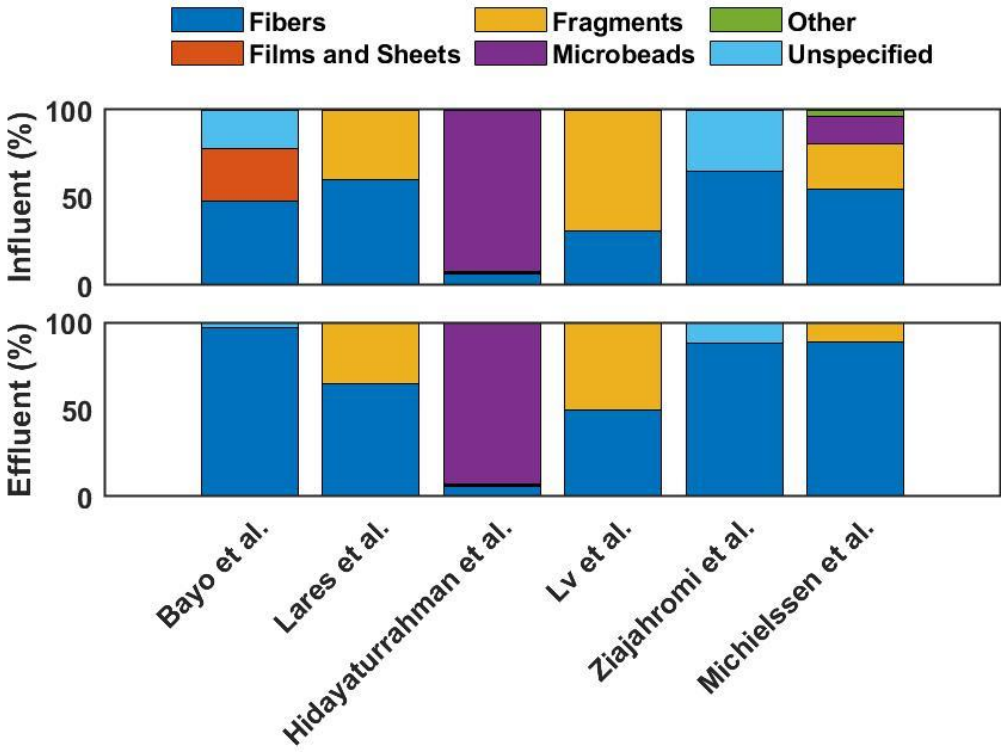

Figure 1.4. Shape distributions for influent and effluent samples from studies reporting both MP shape and concentration.

MPs may have potential impact on membrane processes in terms of fouling and rejection of other contaminants. Li et al [79] found that when 10 MP/L of PVC MPs less than 5 µm in size were added to the feed solution of an MBR, the removal of COD and ammonia was inhibited for several days of operation. As well, MPs caused more significant fouling to the MBR, though majority of the fouling was reversible. As fouling is a significant challenge for MBRs,

understanding how MPs may contribute is crucial to fouling prevention. As well, MPs may have the potential to cause abrasion to the surface of the membrane due to the jagged edges and polymer chemistry of some MPs. As common MP chemistries such as high density polyethylene have higher hardness than common membrane polymers, they could abrade the membrane surface, allowing increased transmission of both MPs and organic contaminants [46]. To date, there have been no studies investigating membrane abrasion due to MPs. All full-scale studies to date have focused solely on the rejection of MPs using membrane systems but it is also important to understand the effects MPs may have on the rejection of organic contaminants which membranes are meant to remove.

1.5.2 Laboratory Scale Studies of Filtration of Microplastics

To date there have been fewer than 10 works investigating membrane filtration of MPs in small scale laboratory studies. These studies provide a more detailed understanding of the interactions between MPs and membranes as they are able to control and analyze parameters such as solution conditions, MP concentration, size, and shape. A challenge in studying membrane filtration of MPs is using particles realistic to MPs found in WWTPs or the environment. Nano- or microparticles that are easily produced or purchase are often spherical and uniform which does not accurately represent MPs, especially MPFs, films, or foams. Ma et al [80] investigated the effects of coagulation using aluminum and iron salts followed by ultrafiltration using polyethylene MP particles, finding that coagulation of natural organic matter in the presence of MPs induced membrane fouling. The aluminum salts induced higher removal efficiencies of MPs due to their larger zeta potential compared to the iron salts and smaller MPs were more easily removed due to coagulation. Larger MPs caused less severe fouling as compared to smaller MPs due to greater roughness in the cake layer. MPs were found to be completely rejected by the membrane in this

study [80]. Enfrin et al [81] studied fouling of an UF membrane using polyethylene MP particles 13 – 690 nm in diameter derived from a commercial facial scrub. They found that the filtration of MPs reduced permeate water flux by 38% over 48h as compared to filtering water without MPs present. This was due to MPs adsorbing onto the surface of the membrane causing pore blockage and cake layer formation [81]. Pizzichetti et al [82] investigated the performance of polycarbonate, cellulose acetate, and polytetrafluoroethylene MF membranes, all with the same nominal pore size of 5 µm, in filtering polyamide and polystyrene MP particles 20 – 300 µm in diameter. All three membranes tested had MP removal efficiencies above 94%. MPs larger than 5 µm were found in the permeate, which the authors hypothesized was caused by membrane abrasion, though they did not provide any additional experimental evidence to support this hypothesis. Some MPs found in the permeate were smaller than those present in the feed which was attributed to MP fragmentation due to mechanical stress [82].

As these works have found that MPs can cause cake layer formation and membrane fouling, there have been two works focusing on preventing membrane fouling due to the adsorption of MPs on the membrane surface. Enfrin et al [83] found that applying a hydrophilic surface coating to a PES UF membrane reduced the adsorption of polyethylene NPs by up to 60%. This was confirmed by extended Derjaguin-Landau-Verwey-Overbeek (XDLVO) theory, which found that the membranes with hydrophilic surface coatings had repulsive interactions with NPs. Polar forces were identified as the predominant interactions contributing to membrane fouling. In a separate work, Enfrin et al [84] applied periodic gas scouring during NP filtration in an attempt to minimize NP adsorption. Gas scouring was found to be more effective for hydrophobic membranes in preventing NP adsorption; no enhancement in permeability was observed for the hydrophilic membranes tested.

Current studies provide an initial look into how MPs interact with membranes when filtered but they do not cover the range of properties that MPs can have, specifically in terms of shape. To date, no studies have investigated the effects of MPFs on membrane filtration at the laboratory scale, despite fibers being a dominant shape in the influent and effluent of many WWTPs MPFs being noted as having lower removal efficiencies as compared to MP fragments. Cai et al [85] have studied the filtration of different MP shapes and sizes using filters that would be used to detect and quantify MPs from WW or environmental samples. The filters tested were made of polycarbonate, nylon, mixed cellulose, cotton fiber, and stainless steel, with pores in the range of 0.45 – 500 µm, depending on filter type. They found that MPFs larger than the nominal pore size were found in the filtrate though the size range of MP fragments was smaller than the nominal pore size for majority of filters. Filter structure was found to have an impact on the retention of MPs as filters with straighter and shorter pores allowed MPFs to pass through more easily than filters with deeper and more tortuous structures [85]. This study provides key results indicating that pore size and membrane structure may impact MP retention. These factors should be investigated using membranes commonly found in WWTPs to better understand how they relate to MP removal.

In general, there are few laboratory studies investigating the filtration of particles that are non-spherical that would provide insight into the filtration of non-spherical MPs. Filtration studies have been conducted using gold nanorods, 35 – 50 nm in length and 12 – 25 nm in diameter, to mimic the filtration of capsular viruses and bacteria. Compared to spherical particles of with the same pore to diameter ratio, capsular particles have been found to have higher rejection due their ability to have different orientations when approaching or inside membrane pores [86][87]. Capsular particles were found to behave similar to spherical particles in terms of rejection when

oriented with the pores of a slit pore membrane [88]. As well, non-spherical particles can change cake layer formation during membrane fouling. Connell et al [89] found that highly branched graphite particles formed a less dense cake layer on the membrane surface as compared to spherical particles or platelets which could stack together more easily, allowing for less hinderance to permeate flux. Though these studies provide insight into how non-spherical MPs may interact with membranes, they differ greatly in terms of particle properties, specifically in terms of particle shape, aspect ratio, and stiffness. Specifically, MPFs are much larger in size, ranging from 20 to 5000 μm in length, and are not rigid like a gold nanorod [ref, microfibers generated…].

1.6 Motivations and Objectives

This work is motivated by the need to better understand the effects of MPFs on membrane filtration. Though in the last two years there have been studies focusing on the filtration of MPs, these studies have only investigated MP fragments which do not encompass the different shapes MPs can have, specifically MPFs. With multiple studies in full scale WWTPs observing MPFs being the dominant shape in both the influent and effluent of membrane systems, it is critical to better understand the impacts of MPFs on membrane filtration. The main goal of this work is to gain a better understanding of how solution conditions, membrane properties, and MPF properties can impact particle rejection and membrane fouling. The specific goals of this project were to:

- Develop a method to create MPFs with different physio-chemical properties to be used in filtration experiments.
- Develop a fundamental understanding of the effects of MPF properties such as size and concentration on membrane performance (e.g. rejection, fouling).

- Investigate the impact of MPFs on filtration using conditions realistic to WWTPs including solution conditions and relevant membranes.

1.7 References

[1] J. J. Klemeš, Y. Van Fan, and P. Jiang, "Plastics: friends or foes? The circularity and plastic waste footprint," *Energy Sources, Part A Recover. Util. Environ. Eff.*, vol. 43, no. 13, pp. 1549–1565, 2021, doi: 10.1080/15567036.2020.1801906.

[2] A. L. Andrady, "Microplastics in the marine environment," *Mar. Pollut. Bull.*, vol. 62, no. 8, pp. 1596–1605, 2011, doi: 10.1016/j.marpolbul.2011.05.030.

[3] R. C. Thompson, C. J. Moore, F. S. V. Saal, and S. H. Swan, "Plastics, the environment and human health: Current consensus and future trends," *Philos. Trans. R. Soc. B Biol. Sci.*, vol. 364, no. 1526, pp. 2153–2166, 2009, doi: 10.1098/rstb.2009.0053.

[4] J. P. da Costa, P. S. M. Santos, A. C. Duarte, and T. Rocha-Santos, "(Nano)plastics in the environment - Sources, fates and effects," *Sci. Total Environ.*, vol. 566–567, pp. 15–26, 2016, doi: 10.1016/j.scitotenv.2016.05.041.

[5] GESMAP, "Sources, fate and effects of microplastics in the marine environment: A global assessment," 2015, [Online]. Available: www.imo.org.

[6] J. Sun, X. Dai, Q. Wang, M. C. M. van Loosdrecht, and B. J. Ni, "Microplastics in wastewater treatment plants: Detection, occurrence and removal," *Water Res.*, vol. 152, pp. 21–37, 2019, doi: 10.1016/j.watres.2018.12.050.

[7] M. Cole, P. Lindeque, C. Halsband, and T. S. Galloway, "Microplastics as contaminants in the marine environment: A review," *Mar. Pollut. Bull.*, vol. 62, no. 12, pp. 2588–2597, 2011, doi: 10.1016/j.marpolbul.2011.09.025.

[8] D. Habib, D. C. Locke, and L. J. Cannone, "Synthetic fibers as indicators of municipal sewage sludge, sludge products, and sewage treatment plant effluents," *Water. Air. Soil Pollut.*, vol. 103, no. 1–4, pp. 1–8, 1998, doi: 10.1023/A:1004908110793.

[9] World Health Organization, "Microplastics in Drinking Water," Geneva, 2019. [Online]. Available: http://library1.nida.ac.th/termpaper6/sd/2554/19755.pdf.

[10] V. Hidalgo-Ruz, L. Gutow, R. C. Thompson, and M. Thiel, "Microplastics in the marine environment: A review of the methods used for identification and quantification," *Environ. Sci. Technol.*, vol. 46, no. 6, pp. 3060–3075, 2012, doi: 10.1021/es2031505.

[11] D. Eerkes-Medrano, R. C. Thompson, and D. C. Aldridge, "Microplastics in freshwater systems: A review of the emerging threats, identification of knowledge gaps and prioritisation of research needs," *Water Res.*, vol. 75, pp. 63–82, 2015, doi: 10.1016/j.watres.2015.02.012.

[12] J. Gago, O. Carretero, A. V. Filgueiras, and L. Viñas, "Synthetic microfibers in the marine environment: A review on their occurrence in seawater and sediments," *Mar. Pollut. Bull.*,

vol. 127, no. July 2017, pp. 365–376, 2018, doi: 10.1016/j.marpolbul.2017.11.070.

[13] Y. Chae and Y. J. An, “Effects of micro- and nanoplastics on aquatic ecosystems: Current research trends and perspectives,” *Mar. Pollut. Bull.*, vol. 124, no. 2, pp. 624–632, 2017, doi: 10.1016/j.marpolbul.2017.01.070.

[14] M. Eriksen *et al.*, “Microplastic pollution in the surface waters of the Laurentian Great Lakes,” *Mar. Pollut. Bull.*, vol. 77, no. 1–2, pp. 177–182, 2013, doi: 10.1016/j.marpolbul.2013.10.007.

[15] S. Allen *et al.*, “Atmospheric transport and deposition of microplastics in a remote mountain catchment,” *Nat. Geosci.*, vol. 12, no. 5, pp. 339–344, 2019, doi: 10.1038/s41561-019-0335-5.

[16] S. Y. Au, T. F. Bruce, W. C. Bridges, and S. J. Klaine, “Responses of Hyalella azteca to acute and chronic microplastic exposures,” *Environ. Toxicol. Chem.*, vol. 34, no. 11, pp. 2564–2572, 2015, doi: 10.1002/etc.3093.

[17] M. Cole *et al.*, “Microplastic ingestion by zooplankton,” *Environ. Sci. Technol.*, vol. 47, no. 12, pp. 6646–6655, 2013, doi: 10.1021/es400663f.

[18] A. J. R. Watts, M. A. Urbina, S. Corr, C. Lewis, and T. S. Galloway, “Ingestion of Plastic Microfibers by the Crab Carcinus maenas and Its Effect on Food Consumption and Energy Balance,” *Environ. Sci. Technol.*, vol. 49, no. 24, pp. 14597–14604, 2015, doi: 10.1021/acs.est.5b04026.

[19] M. Mohsen, L. Zhang, L. Sun, C. Lin, Q. Wang, and H. Yang, “Microplastic fibers transfer from the water to the internal fluid of the sea cucumber Apostichopus japonicus,” *Environ. Pollut.*, vol. 257, 2020, doi: 10.1016/j.envpol.2019.113606.

[20] J. B. Koongolla *et al.*, “Occurrence of microplastics in gastrointestinal tracts and gills of fish from Beibu Gulf, South China Sea,” *Environ. Pollut.*, vol. 258, p. 113734, 2020, doi: 10.1016/j.envpol.2019.113734.

[21] A. Rebelein, I. Int-Veen, U. Kammann, and J. P. Scharsack, “Microplastic fibers — Underestimated threat to aquatic organisms?,” *Sci. Total Environ.*, vol. 777, p. 146045, 2021, doi: 10.1016/j.scitotenv.2021.146045.

[22] E. L. Teuten *et al.*, “Transport and release of chemicals from plastics to the environment and to wildlife,” *Philos. Trans. R. Soc. B Biol. Sci.*, vol. 364, no. 1526, pp. 2027–2045, 2009, doi: 10.1098/rstb.2008.0284.

[23] M. A. Browne, S. J. Niven, T. S. Galloway, S. J. Rowland, and R. C. Thompson, “Microplastic moves pollutants and additives to worms, reducing functions linked to health and biodiversity,” *Curr. Biol.*, vol. 23, no. 23, pp. 2388–2392, 2013, doi: 10.1016/j.cub.2013.10.012.

[24] M. Manabe, N. Tatarazako, and M. Kinoshita, “Uptake, excretion and toxicity of nano-sized latex particles on medaka (Oryzias latipes) embryos and larvae,” *Aquat. Toxicol.*, vol. 105, no. 3–4, pp. 576–581, 2011, doi: 10.1016/j.aquatox.2011.08.020.

[25] C. B. Jeong *et al.*, “Microplastic Size-Dependent Toxicity, Oxidative Stress Induction, and

p-JNK and p-p38 Activation in the Monogonont Rotifer (Brachionus koreanus)," *Environ. Sci. Technol.*, vol. 50, no. 16, pp. 8849–8857, 2016, doi: 10.1021/acs.est.6b01441.

[26] J. E. Ward and D. J. Kach, "Marine aggregates facilitate ingestion of nanoparticles by suspension-feeding bivalves," *Mar. Environ. Res.*, vol. 68, no. 3, pp. 137–142, 2009, doi: 10.1016/j.marenvres.2009.05.002.

[27] E. Oberdörster, "Manufactured nanomaterials (fullerenes, C60) induce oxidative stress in the brain of juvenile largemouth bass," *Environ. Health Perspect.*, vol. 112, no. 10, pp. 1058–1062, 2004, doi: 10.1289/ehp.7021.

[28] P. Farrell and K. Nelson, "Trophic level transfer of microplastic: Mytilus edulis (L.) to Carcinus maenas (L.)," *Environ. Pollut.*, vol. 177, pp. 1–3, 2013, doi: 10.1016/j.envpol.2013.01.046.

[29] C. Walkinshaw, P. K. Lindeque, R. Thompson, T. Tolhurst, and M. Cole, "Microplastics and seafood: lower trophic organisms at highest risk of contamination," *Ecotoxicol. Environ. Saf.*, vol. 190, no. December 2019, p. 110066, 2020, doi: 10.1016/j.ecoenv.2019.110066.

[30] D. D. A. Miranda and G. F. De Carvalho-souza, "Are we eating plastic-ingesting fi sh ?," *Mar. Pollut. Bull.*, vol. 103, no. 1–2, pp. 109–114, 2016, doi: 10.1016/j.marpolbul.2015.12.035.

[31] K. Mattsson, E. V. Johnson, A. Malmendal, S. Linse, L. A. Hansson, and T. Cedervall, "Brain damage and behavioural disorders in fish induced by plastic nanoparticles delivered through the food chain," *Sci. Rep.*, vol. 7, no. 1, pp. 1–7, 2017, doi: 10.1038/s41598-017-10813-0.

[32] L. Van Cauwenberghe and C. R. Janssen, "Microplastics in bivalves cultured for human consumption," *Environ. Pollut.*, vol. 193, pp. 65–70, 2014, doi: 10.1016/j.envpol.2014.06.010.

[33] A. I. Catarino, V. Macchia, W. G. Sanderson, R. C. Thompson, and T. B. Henry, "Low levels of microplastics (MP) in wild mussels indicate that MP ingestion by humans is minimal compared to exposure via household fibres fallout during a meal," *Environ. Pollut.*, vol. 237, pp. 675–684, 2018, doi: 10.1016/j.envpol.2018.02.069.

[34] S. A. Mason, V. G. Welch, and J. Neratko, "Synthetic Polymer Contamination in Bottled Water," *Front. Chem.*, vol. 6, no. September, 2018, doi: 10.3389/fchem.2018.00407.

[35] V. C. Shruti, F. Pérez-Guevara, I. Elizalde-Martínez, and G. Kutralam-Muniasamy, "First study of its kind on the microplastic contamination of soft drinks, cold tea and energy drinks - Future research and environmental considerations," *Sci. Total Environ.*, vol. 726, p. 138580, 2020, doi: 10.1016/j.scitotenv.2020.138580.

[36] L. M. Hernandez, E. G. Xu, H. C. E. Larsson, R. Tahara, V. B. Maisuria, and N. Tufenkji, "Plastic Teabags Release Billions of Microparticles and Nanoparticles into Tea," *Environ. Sci. Technol.*, vol. 53, no. 21, pp. 12300–12310, 2019, doi: 10.1021/acs.est.9b02540.

[37] R. Dris *et al.*, "A first overview of textile fibers, including microplastics, in indoor and

outdoor environments," *Environ. Pollut.*, vol. 221, pp. 453–458, 2017, doi: 10.1016/j.envpol.2016.12.013.

[38] J. Gasperi *et al.*, "Microplastics in air: Are we breathing it in?," *Curr. Opin. Environ. Sci. Heal.*, vol. 1, pp. 1–5, 2018, doi: 10.1016/j.coesh.2017.10.002.

[39] L. N. Vandenberg *et al.*, "Hormones and endocrine-disrupting chemicals: Low-dose effects and nonmonotonic dose responses," *Endocr. Rev.*, vol. 33, no. 3, pp. 378–455, 2012, doi: 10.1210/er.2011-1050.

[40] B. Koelmans and S. Pahl, *A Scientific Perspective on Microplastics in Nature and Society*, no. 4. 2019.

[41] M. A. Browne *et al.*, "Accumulation of microplastic on shorelines woldwide: Sources and sinks," *Environ. Sci. Technol.*, vol. 45, no. 21, pp. 9175–9179, 2011, doi: 10.1021/es201811s.

[42] S. A. Carr, J. Liu, and A. G. Tesoro, "Transport and fate of microplastic particles in wastewater treatment plants," *Water Res.*, vol. 91, pp. 174–182, 2016, doi: 10.1016/j.watres.2016.01.002.

[43] J. Talvitie, A. Mikola, O. Setälä, M. Heinonen, and A. Koistinen, "How well is microlitter purified from wastewater? – A detailed study on the stepwise removal of microlitter in a tertiary level wastewater treatment plant," *Water Res.*, vol. 109, pp. 164–172, 2017, doi: 10.1016/j.watres.2016.11.046.

[44] F. Murphy, C. Ewins, F. Carbonnier, and B. Quinn, "Wastewater Treatment Works (WwTW) as a Source of Microplastics in the Aquatic Environment," *Environ. Sci. Technol.*, vol. 50, no. 11, pp. 5800–5808, 2016, doi: 10.1021/acs.est.5b05416.

[45] S. M. Mintenig, I. Int-Veen, M. G. J. Löder, S. Primpke, and G. Gerdts, "Identification of microplastic in effluents of waste water treatment plants using focal plane array-based micro-Fourier-transform infrared imaging," *Water Res.*, vol. 108, pp. 365–372, 2017, doi: 10.1016/j.watres.2016.11.015.

[46] M. Enfrin, L. F. Dumée, and J. Lee, "Nano/microplastics in water and wastewater treatment processes – Origin, impact and potential solutions," *Water Res.*, vol. 161, pp. 621–638, 2019, doi: 10.1016/j.watres.2019.06.049.

[47] V. S. Koutnik *et al.*, "Unaccounted Microplastics in Wastewater Sludge: Where Do They Go?," *ACS ES&T Water*, vol. 1, no. 5, pp. 1086–1097, 2021, doi: 10.1021/acsestwater.0c00267.

[48] F. Corradini, P. Meza, R. Eguiluz, F. Casado, E. Huerta-Lwanga, and V. Geissen, "Evidence of microplastic accumulation in agricultural soils from sewage sludge disposal," *Sci. Total Environ.*, vol. 671, pp. 411–420, 2019, doi: 10.1016/j.scitotenv.2019.03.368.

[49] P. He, L. Chen, L. Shao, H. Zhang, and F. Lü, "Municipal solid waste (MSW)landfill: A source of microplastics? -Evidence of microplastics in landfill leachate," *Water Res.*, vol. 159, pp. 38–45, 2019, doi: 10.1016/j.watres.2019.04.060.

[50] J. Crossman, R. R. Hurley, M. Futter, and L. Nizzetto, “Transfer and transport of microplastics from biosolids to agricultural soils and the wider environment,” *Sci. Total Environ.*, vol. 724, p. 138334, 2020, doi: 10.1016/j.scitotenv.2020.138334.

[51] F. De Falco, E. Di Pace, M. Cocca, and M. Avella, “The contribution of washing processes of synthetic clothes to microplastic pollution,” *Sci. Rep.*, no. January, pp. 1–11, 2019, doi: 10.1038/s41598-019-43023-x.

[52] J. Boucher and D. Friot, *Primary Microplastics in the Oceans: a Global Evaluation of Sources*, vol. 1, no. 1. 2017.

[53] I. E. Napper, A. Bakir, S. J. Rowland, and R. C. Thompson, “Characterisation, quantity and sorptive properties of microplastics extracted from cosmetics,” *Mar. Pollut. Bull.*, vol. 99, no. 1–2, pp. 178–185, 2015, doi: 10.1016/j.marpolbul.2015.07.029.

[54] N. Zhang, Y. Bin Li, H. R. He, J. F. Zhang, and G. S. Ma, “You are what you eat: Microplastics in the feces of young men living in Beijing,” *Sci. Total Environ.*, vol. 767, p. 144345, 2021, doi: 10.1016/j.scitotenv.2020.144345.

[55] J. R. Jambeck *et al.*, “Plastic waste inputs from land into the ocean,” vol. 347, no. 6223, pp. 768–771, 2021.

[56] D. K. A. Barnes, F. Galgani, R. C. Thompson, and M. Barlaz, “Accumulation and fragmentation of plastic debris in global environments,” *Philos. Trans. R. Soc. B Biol. Sci.*, vol. 364, no. 1526, pp. 1985–1998, 2009, doi: 10.1098/rstb.2008.0205.

[57] M. Kazour, S. Terki, K. Rabhi, S. Jemaa, G. Khalaf, and R. Amara, “Sources of microplastics pollution in the marine environment: Importance of wastewater treatment plant and coastal landfill,” *Mar. Pollut. Bull.*, vol. 146, pp. 608–618, 2019, doi: 10.1016/j.marpolbul.2019.06.066.

[58] A. Sonune and R. Ghate, “Developments in wasetwater treatment methods,” *Desalination*, vol. 167, no. 3, pp. 55–63, 2004.

[59] M. Takht Ravanchi, T. Kaghazchi, and A. Kargari, “Application of membrane separation processes in petrochemical industry: a review,” *Desalination*, vol. 235, no. 1–3, pp. 199–244, 2009, doi: 10.1016/j.desal.2007.10.042.

[60] B. Van Der Bruggen, C. Vandecasteele, T. Van Gestel, W. Doyenb, and R. Leysenb, “A Review of Pressure-Driven Membrane Processes in Wastewater Treatment and Drinking Water Production,” *Environ. Prog.*, vol. 22, no. 1, pp. 46–56, 2003.

[61] E. O. Ezugbe and S. Rathilal, “Membrane technologies in wastewater treatment: A review,” *Membranes (Basel).*, vol. 10, no. 5, 2020, doi: 10.3390/membranes10050089.

[62] M. Raffin, E. Germain, and S. Judd, “Wastewater polishing using membrane technology: A review of existing installations,” *Environ. Technol. (United Kingdom)*, vol. 34, no. 5, pp. 617–627, 2013, doi: 10.1080/09593330.2012.710385.

[63] E. Alonso, A. Santos, G. J. Solis, and P. Riesco, “On the feasibility of urban wastewater tertiary treatment by membranes: A comparative assessment,” *Desalination*, vol. 141, no. 1, pp. 39–51, 2001, doi: 10.1016/S0011-9164(01)00387-3.

[64] H. Lin *et al.*, “Membrane bioreactors for industrial wastewater treatment: A critical review,” *Crit. Rev. Environ. Sci. Technol.*, vol. 42, no. 7, pp. 677–740, 2012, doi: 10.1080/10643389.2010.526494.

[65] P. Le-Clech, V. Chen, and T. A. G. Fane, “Fouling in membrane bioreactors used in wastewater treatment,” *J. Memb. Sci.*, vol. 284, no. 1–2, pp. 17–53, 2006, doi: 10.1016/j.memsci.2006.08.019.

[66] T. Melin *et al.*, “Membrane bioreactor technology for wastewater treatment and reuse,” *Desalination*, vol. 187, no. 1–3, pp. 271–282, 2006, doi: 10.1016/j.desal.2005.04.086.

[67] J. Talvitie, A. Mikola, A. Koistinen, and O. Setälä, “Solutions to microplastic pollution – Removal of microplastics from wastewater effluent with advanced wastewater treatment technologies,” *Water Res.*, vol. 123, pp. 401–407, 2017, doi: 10.1016/j.watres.2017.07.005.

[68] J. Bayo, J. López-Castellanos, and S. Olmos, “Membrane bioreactor and rapid sand filtration for the removal of microplastics in an urban wastewater treatment plant,” *Mar. Pollut. Bull.*, vol. 156, no. March, p. 111211, 2020, doi: 10.1016/j.marpolbul.2020.111211.

[69] S. Olmos, J. López-Castellanos, and J. Bayo, “Are advanced wastewater treatment technologies a solution for total removal of microplastics in treated effluents?,” *WIT Trans. Ecol. Environ.*, vol. 229, pp. 109–116, 2019, doi: 10.2495/WRM190111.

[70] A. Foglia *et al.*, “Anaerobic membrane bioreactor for urban wastewater valorisation: Operative strategies and fertigation reuse,” *Chem. Eng. Trans.*, vol. 74, no. November 2018, pp. 247–252, 2019, doi: 10.3303/CET1974042.

[71] X. Lv, Q. Dong, Z. Zuo, Y. Liu, X. Huang, and W. M. Wu, “Microplastics in a municipal wastewater treatment plant: Fate, dynamic distribution, removal efficiencies, and control strategies,” *J. Clean. Prod.*, vol. 225, pp. 579–586, 2019, doi: 10.1016/j.jclepro.2019.03.321.

[72] S. Ziajahromi, P. A. Neale, L. Rintoul, and F. D. L. Leusch, “Wastewater treatment plants as a pathway for microplastics: Development of a new approach to sample wastewater-based microplastics,” *Water Res.*, vol. 112, pp. 93–99, 2017, doi: 10.1016/j.watres.2017.01.042.

[73] H. Hidayaturrahman and T. G. Lee, “A study on characteristics of microplastic in wastewater of South Korea: Identification, quantification, and fate of microplastics during treatment process,” *Mar. Pollut. Bull.*, vol. 146, no. July, pp. 696–702, 2019, doi: 10.1016/j.marpolbul.2019.06.071.

[74] M. R. Michielssen, E. R. Michielssen, J. Ni, and M. B. Duhaime, “Fate of microplastics and other small anthropogenic litter (SAL) in wastewater treatment plants depends on unit processes employed,” *Environ. Sci. Water Res. Technol.*, vol. 2, no. 6, pp. 1064–1073, 2016, doi: 10.1039/c6ew00207b.

[75] H. A. Leslie, S. H. Brandsma, M. J. M. van Velzen, and A. D. Vethaak, “Microplastics en route: Field measurements in the Dutch river delta and Amsterdam canals, wastewater

treatment plants, North Sea sediments and biota," *Environ. Int.*, vol. 101, pp. 133–142, 2017, doi: 10.1016/j.envint.2017.01.018.

[76] C. Baresel *et al.*, "Membrane Bioreactor Processes to Meet Todays and Future Municipal Sewage Treatment Requirements?," *Int. J. Water Wastewater Treat.*, vol. 3, no. 2, 2017, doi: 10.16966/2381-5299.140.

[77] C. Baresel, M. Harding, and J. Fang, "Ultrafiltration/granulated active carbon-biofilter: Efficient removal of a broad range of micropollutants," *Appl. Sci.*, vol. 9, no. 4, 2019, doi: 10.3390/app9040710.

[78] M. Lares, M. C. Ncibi, M. Sillanpää, and M. Sillanpää, "Occurrence, identification and removal of microplastic particles and fibers in conventional activated sludge process and advanced MBR technology," *Water Res.*, vol. 133, pp. 236–246, 2018, doi: 10.1016/j.watres.2018.01.049.

[79] L. Li, D. Liu, K. Song, and Y. Zhou, "Performance evaluation of MBR in treating microplastics polyvinylchloride contaminated polluted surface water," *Mar. Pollut. Bull.*, vol. 150, no. November 2019, pp. 1–6, 2020, doi: 10.1016/j.marpolbul.2019.110724.

[80] B. Ma, W. Xue, C. Hu, H. Liu, J. Qu, and L. Li, "Characteristics of microplastic removal via coagulation and ultrafiltration during drinking water treatment," *Chem. Eng. J.*, vol. 359, no. November 2018, pp. 159–167, 2019, doi: 10.1016/j.cej.2018.11.155.

[81] M. Enfrin, J. Lee, P. Le-Clech, and L. F. Dumée, "Kinetic and mechanistic aspects of ultrafiltration membrane fouling by nano- and microplastics," *J. Memb. Sci.*, vol. 601, no. January, 2020, doi: 10.1016/j.memsci.2020.117890.

[82] A. R. P. Pizzichetti, C. Pablos, C. Álvarez-Fernández, K. Reynolds, S. Stanley, and J. Marugán, "Evaluation of membranes performance for microplastic removal in a simple and low-cost filtration system," *Case Stud. Chem. Environ. Eng.*, vol. 3, no. December 2020, p. 100075, 2021, doi: 10.1016/j.cscee.2020.100075.

[83] M. Enfrin, J. Wang, A. Merenda, L. F. Dumée, and J. Lee, "Mitigation of membrane fouling by nano/microplastics via surface chemistry control," *J. Memb. Sci.*, vol. 633, no. March, 2021, doi: 10.1016/j.memsci.2021.119379.

[84] M. Enfrin, J. Lee, A. G. Fane, and L. F. Dumée, "Mitigation of membrane particulate fouling by nano/microplastics via physical cleaning strategies," *Sci. Total Environ.*, vol. 788, p. 147689, 2021, doi: 10.1016/j.scitotenv.2021.147689.

[85] H. Cai, M. Chen, Q. Chen, F. Du, J. Liu, and H. Shi, "Microplastic quantification affected by structure and pore size of filters," *Chemosphere*, vol. 257, p. 127198, 2020, doi: 10.1016/j.chemosphere.2020.127198.

[86] B. Agasanapura, R. E. Baltus, C. T. Tanneru, and S. Chellam, "Effect of electrostatic interactions on rejection of capsular and spherical particles from porous membranes: Theory and experiment," *J. Colloid Interface Sci.*, vol. 448, pp. 492–500, 2015, doi: 10.1016/j.jcis.2015.02.016.

[87] A. Delavari, B. Agasanapura, and R. E. Baltus, "The effect of particle rotation on the

motion and rejection of capsular particles in slit pores," *AIChE J.*, vol. 64, no. 7, pp. 2828–2836, 2018, doi: 10.1002/aic.16132.

[88] R. E. Baltus, A. R. Badireddy, W. Xu, and S. Chellam, "Analysis of configurational effects on hindered convection of nonspherical bacteria and viruses across microfiltration membranes," *Ind. Eng. Chem. Res.*, vol. 48, no. 5, pp. 2404–2413, 2009, doi: 10.1021/ie800579e.

[89] H. Connell, J. Zhu, and A. Bassi, "Effect of particle shape on crossflow filtration flux," *J. Memb. Sci.*, vol. 153, no. February 1998, 1999.

Chapter 2: Assessment of solution and membrane properties on microplastic fiber filtration

2.1 Introduction

Microplastics (MPs) have become ubiquitous in the environment being found in freshwater [1] and marine environments [2][3][4] as well as drinking water sources [5]. MPs can originate from primary sources, where they have been manufactured to be of microscopic size or secondary sources, as the result of the fragmentation of larger plastics [3]. MPs vary significantly in their shape (fragments, fibers, films, etc), size, and chemistry (polyethylene, polystyrene, polyethylene terephthalate, etc) [4][6]. The heterogeneity of their properties makes MPs difficult to detect, quantify, and remove [7]. These small plastics particles pose a significant threat to aquatic life as the ingestion of MPs can cause adverse effects on the development, behaviour, and mortality of aquatic organisms [4][8][9]. Toxic organic compounds are able to easily adsorb onto MPs due to their high surface area and hydrophobicity [10]. These toxic pollutants have the potential to transfer to aquatic organisms and enter into the food web with the potential to reach larger animals including humans; the potential impacts of MPs on human health are to-date largely unknown [4][8][11][5]. Wastewater treatment plant (WWTP) effluents have been found to be a significant entry point for MPs into the environment [12]. MPs can enter WWTPs as microbeads from personal care products, fibers released from the laundering of synthetic textiles, and the breakdown of macroplastics [12][13], among other routes. While primary and secondary treatment steps are effective in removing the majority of MPs [7], treated effluents may contain up to 450 MPs/L causing significant contamination of aquatic ecosystems due to the high volumes of effluent released [12][13][7]. Ultrafiltration (UF) and microfiltration (MF) membrane systems used in some WWTPs have the potential to be effective for MP removal due to the small size of the membrane pores compared to the size of MPs [14][15][7].

Current literature studying MP removal in WWTPs has investigated the effectiveness of filtration systems such as disc filters, membrane bioreactors (MBRs), and tertiary treatment systems using UF and reverse osmosis membranes [16]–[29]. Each of these studies had significant variation in the influent in terms of MP characteristics. as well as inconsistency in reporting of both the properties of the microplastics and the membrane filtration system, making it difficult to draw conclusions about membrane effectiveness between studies. Furthermore, the focus of these works was on the filtration of MPs with regards to the overall process rather than the detailed effects MPs may have on the membrane itself, resulting in a limited understanding of the MP-membrane interactions leading to vastly different removal properties for similar systems; for instance, two studies investigating the removal of MPs using MBRs with similar feed concentrations (60 MP/L and 68 MP/L) reported significantly different removal efficiencies (99% and 25% respectively) [16][18]. Studies investigating the interactions between MPs and membrane systems in more detail are necessary to determine how the properties of MPs and membranes impact MP filtration. Lab-scale studies offer more definite conclusions regarding the interactions between plastic particles and membranes; however the majority of such studies in the current literature use uniform spherical nanoparticles in buffer solutions that are not representative of the variation in properties of MPs and solution conditions in WWTPs[31] [32][32].

Few studies, all published within the last two years and all focused on MP fragments, have examined the impacts of realistic MPs on membrane systems in detail [33][10][34]. Pizzichetti et al [34] found that polystyrene and polyamide particles purchased from a materials supplier, sieved and milled to be 20-300 μm in diameter, were able to pass through MF membranes due to MP fragmentation and membrane abrasion during the filtration process. Enfrin et al [33] investigated the filtration of polyethylene from a commercial facial scrub MPs 13 – 690 nm in diameter through

a UF membrane, finding that MPs reduced permeate water flux by 38% over a 48h experiment and adsorbed onto the surface of the membrane. Ma et al found that smaller PE particles, purchased from a supplier, caused more severe fouling to a UF membrane than larger particles. When combined with coagulation, large MPs were able to disrupt the cake layer forming during filtration [10]. However, while MP fibers (MPFs) have been found to represent up to 60% of MPs in WW influents [22][23][16] and effluents [19][23][24][27][25] of WWTPs, to-date no studies have been conducted on MPF removal specifically, despite their noted lower removal efficiencies as compared to MPs of other shapes such as fragments and microbeads [18], [23]–[26]. The only current studies using non-spherical particles use gold nanorods and have reported higher rejection for nanorods compared to spherical particles with the same diameter and volume [35][36]. However, these studies may have limited applicability to MPFs due to the significant difference in shape, stiffness, and chemistry between MPFs and gold nanorods; indeed nanorods are much stiffer and have much lower length and aspect ratio compared to MPFs, which can be 10 μm to 5 mm in length [4][16][37].

In this work, we investigated the impacts of MPFs on membrane filtration using MF membranes. Model MPFs were fabricated based on the MP-relevant material polystyrene by combining electrospinning with a cryostat cutting process [38]. The effects of MPF concentration and membrane pore size on filtration performance were investigated using permeability and transmembrane pressure measurements, both in Milli-Q water and wastewater from a municipal WWTP. We particularly aim to understand the effect of the solution conditions on the interactions between the MPFs and membrane to allow for the improved design and operation of membrane filtration systems, ultimately leading to reductions in the discharge of MPFs into the environment.

2.2 Materials and Methods

2.2.1 Microplastic Fiber Synthesis

Polystyrene (PS, M_w ~192000 g/mol) and N,N,dimethylformamide (DMF) were purchased from Sigma Aldrich. PS was dissolved in DMF with several drops of nitric acid (3 drops from a glass Pasteur pipette added to 10 mL of polymer solution) to create a 30 wt% polymer solution [39] [40]. This solution was loaded into a 1 mL syringe with a 25-gauge blunt needle that was loaded into a syringe pump that enabled extrusion of the solution at a rate of 2 µL/min. The polymer solution was electrospun by applying a voltage of 20 kV between the needle and a rotating drum collector, 3 cm in diameter, using a high voltage power supply. The electrospun fibers were collected on a piece of aluminum foil attached to the rotating drum collector for 2 hours, which rotated at a speed of 2000 rpm. The distance between the needle and the collector was 10 cm. The polymer concentration, applied voltage, needle-to-collector distance, and polymer feed rate were adapted from Lee et al [39] and Jarusuwannapoom and Hongrojjanawiwat [40] and optimized to ensure fibers had minimal beads. An image of the electrospun fiber mat is shown in Figure 2.S1. To cut the MPFs, a cryostat cutting protocol was used [38]. The fiber mat was coated in freezing compound (Tissue-Tek) and frozen for at least 20 minutes in a -20ºC freezer. The frozen fiber mat was then cut into sections and frozen together into a block using the freezing compound. This block was then cut using a cryostat (Leica CM3050) at a cut setting of 100 µm. The cut sections were placed in a glass bottle which was filled with room temperature Milli-Q water and mixed using a magnetic stir plate overnight to thaw and separate the MPFs. The freezing compound was removed by filtering the MPF solution through a Whatman 41 filter paper and gently removing the MPFs that collected on top of the filter paper. The collected MPFs were weighed and suspended in a known volume of Milli-Q water to create a stock suspension of known concentration The MPF stock suspension was sonicated for 30 minutes using an ultrasonic bath (Branson). A more in depth

MPF synthesis protocol is provided in Appendix A. To prepare MPF suspensions for filtration experiments, MPF stock solution was diluted to a volume of 160 mL in either Milli-Q water or wastewater (WW) to achieve MPF concentrations of 5, 10, 50 or 100 mg/mL. This solution was placed on a rocking tray for 10-20 minutes to ensure MPFs were evenly dispersed in the suspension then sonicated in an ultrasonic bath for 1 hour to ensure disaggregation.

2.2.2 Municipal Wastewater

Municipal (WW) in the form of secondary clarifier effluent was obtained from the Dundas Wastewater Treatment Plant (Hamilton, ON). Any visible solids were allowed to settle and the supernatant was used to suspend MPFs in filtration experiments. The WW was characterized using total solids (TS) content, total carbon (TC), total organic carbon (TOC), chemical oxygen demand (COD), and conductivity. The TS was measured by heating a known mass of WW at 104 ^{o}C in an aluminium dish to evaporate the water. The solids concentration was calculated as the difference between the initial and final mass. The TC and TOC was measured using a Shimadzu TOC-L instrument with a calibration curve based on potassium hydrogen phthalate standard. COD was measured using standard Hach HR COD vials and a spectrophotometer (Hach DR 3900) following the manufacturer's method. The conductivity of the WW was determined using a conductivity probe (Hanna Instruments HI5522). The average and standard deviation of each property measured is shown in Table 2.1.

Table 2.1. Properties of WW used for suspending MPFs in filtration experiments.

TS (mg/L)	TC (mg/L)	TOC (mg/L)	COD (mg/L)	Conductivity (µS/cm)
847 ± 115	30 ± 1	5.2 ± 0.3	56 ± 9	1084 ± 18

2.2.3 Filtration Experiments

Durapore PVDF membranes 13 mm in diameter with nominal pore sizes of 0.22 µm (purchased from Sigma Aldrich) and 5 µm (donated by Millipore) were used in filtration experiments. As shown in Figure 2.1, a custom filtration set-up employing a multi-channel peristaltic pump (Cole-Parmer) was used to conduct three filtration experiments in parallel. An acetal (polyoxymethylene copolymer) block fitted with three separate channels was used to house individual membrane holders (Cole-Parmer). Three USB pressure transducers (Omega PX409) were screwed into the acetal (polyoxymethylene copolymer) block to monitor transmembrane pressure (TMP) for each membrane during the experiments.

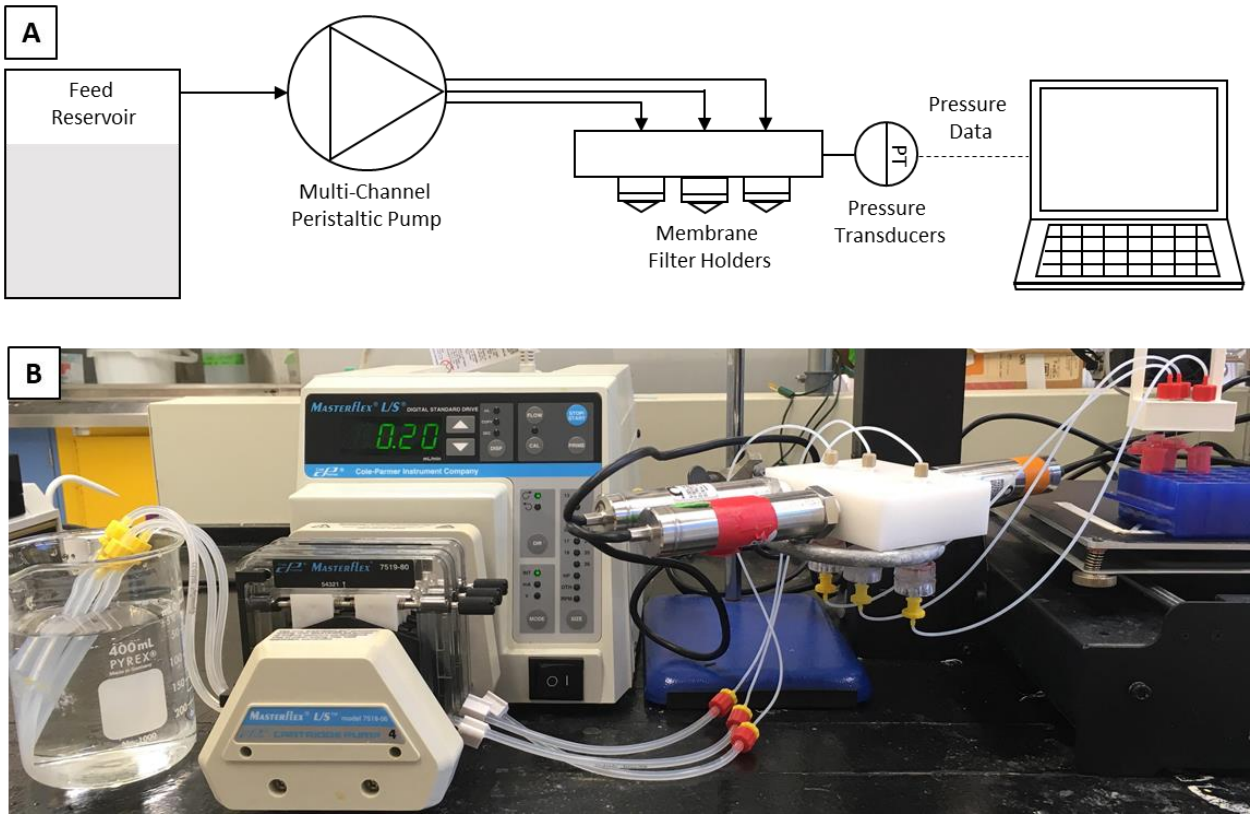

Figure 2.1. Diagram (A) and image (B) of membrane filtration set-up.

Before conducting the filtration experiments, the membranes were placed inside of the membrane holders and 20 mL of Milli-Q water was passed through them with a syringe to ensure wetting. Once wetted, the membrane holders were attached to the filtration set up and Milli-Q water was passed through the membranes at 450 L/m^2/h (LMH) for 10 minutes or until constant TMP was achieved. Hydraulic permeability (L_p) was measured prior to the filtration experiment and calculated using Eq. 1, where J is the flux of Milli-Q water (LMH) and TMP is the transmembrane pressure (bar). Permeability was measured using six flux values between 120 – 360 LMH and repeated twice. The true permeate flux was determined by collecting the permeate in a 48 well plate for each membrane and measuring the volume collected over time by measuring absorbance at 977 nm using a plate reader (Tecan) [41].

$$L_p = \frac{J}{TMP} \quad (1)$$

Following the initial permeability measurement, the prepared MPF suspension was filtered through the membranes for 4 hours at 225 ± 21 LMH (where the ± represents standard deviation). Due to flowrate variation between the different pump channels, the flux from each channel was measured throughout filtration experiment. This flux was chosen as it is within the operating range of permeate fluxes used for MF membranes in WWTPs [42]. Filtration experiments were conducted for 4 hours as this run time at a MPF concentration of 10 mg/L roughly corresponds to the amount of MPs a membrane system in a WWTP would encounter [43]. TMP was logged continuously and 2 mL permeate samples were collected every hour during the filtration experiment. Following MPF filtration, the membrane holders were removed from the set-up and the solution on top of the membrane was removed using a pipette. The filtration set-up was rinsed thoroughly with Milli-Q water before reattaching the membrane holders. The permeability was then measured using Milli-Q water using the same process as the initial permeability measurement.

Following, the membranes were carefully removed from the membrane holders to be used for microscopy analysis. At least two sets of triplicate experiments were performed for each experimental condition to yield six replicates.

2.2.4 Microscopy Analysis

MPFs were imaged using an Olympus inverted IX51 microscope with a QIMaging Retiga 2000R camera to determine their size and concentration. 0.5 mL of MPF solution from diluted fiber stock solutions or filtration experiment samples were pipetted into a 24 well plate and dried in an oven at 60^{o}C. For each filtration experiment, one 0.5 mL sample was analyzed for each permeate sample collected. The dried samples were imaged, and ImageJ Analysis Software was used to determine the length and diameter of 10-20 images in each sample (depending on the number of MPFs present).

Membranes were imaged following MPF filtration using a JEOL 7000F field-emission scanning electron microscope (SEM). Small sections were cut from the center of the membrane after allowing them to dry completely at room temperature. The membrane sections were mounted on aluminium SEM stubs using carbon tape, sputter-coated with a 5 nm platinum coating and imaged using a 1 kV acceleration voltage.

2.2 Results

2.3.1 Characterization of Microplastic Fibers

Figure 2.2b shows the PS MPFs created using the electrospinning and cryostat cutting method. PS was chosen as the polymer for the MPFs as it has a well documented electrospinning procedure and is a polymer commonly found in MP samples [17][29]. The MPFs have an average length of 73 ± 48 μm and an average diameter of 0.52 ± 0.08 μm (where the ± represents standard deviation). While the length distribution is relatively broad, as shown in Figure 2.2a, this breadth was found

to be acceptable for this study as MPFs entering WWTPs also vary significantly in length, from 10 µm to 5 mm [16]. The majority of MPFs were found to have lengths of 10-80 µm and length : diameter aspect ratios of 40-160; such fibers are more realistic to MP fibers generated from synthetic textiles, although the MPFs produced have smaller diameters compared to those from synthetic textiles (12- 16 µm in diameter) [37]. Though the diameter of the model MPFs is smaller than MPFs generated from synthetic textiles, the unit operations in WWTPs can lead to fragmentation of MPs, resulting in smaller MPs [14].

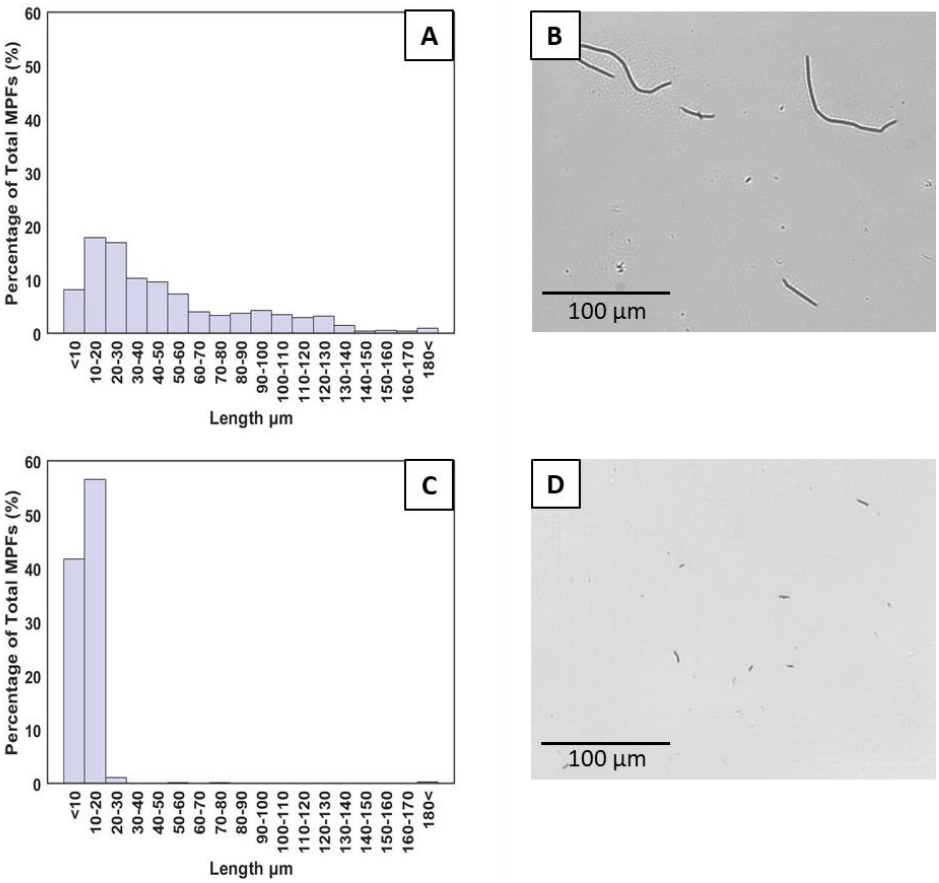

Figure 2.2. Histograms of feed (A) and permeate (C) MPF length and images of feed (B) and permeate (D) samples from experiments filtering 10 mg/L MPFs suspended in Milli-Q water through a 5 µm membrane.

2.3.2 Effect of MPF Concentration

Filtration experiments using concentrations ranging from 5-100 mg/L of MPFs suspended in Milli-Q water were conducted using a 0.22 µm PVDF membrane. Figure 2.3a shows the initial

(Lp0) and final (Lpf) permeability measurements for each MPF concentration tested. For all concentrations, there is minimal change between the initial and final permeability, indicating that significant membrane fouling is not occurring. The difference between initial and final permeability was shown to be not significantly different using a paired Student's t-test (p-values >0.05) for all concentrations except for 5 mg/L (p-value = 0.013). Despite having a statistically significant difference between initial and final permeability, there is minimal evidence of fouling as the permeability drop was small and could have been caused by membrane compaction. This is confirmed by the TMP profiles, shown in Figure 2.S2, which remain fairly constant during the 4-hour experiment for all concentrations tested. Figure 2.3b-f show SEM images of the membranes following the filtration of each MPF concentration as well as the native membrane. For each concentration, MPFs appear to be depositing on the surface of the membrane and not entering into the membrane pores, which is expected as the diameter of the MPFs exceeds the nominal pore size of the membrane.

As the feed concentration of MPFs increases, more MPFs are deposited on the membrane surface but the pore structure of the membrane remains visible for all concentrations tested. As many of the pores remain unblocked by the MPFs, there is limited resistance to flow through the membrane, corresponding to minimal change in permeability and TMP during each experiment. More significant areas of pore blockage are seen for the 100 mg/L concentration where clumps of MPFs are observed on the membrane surface; however, these areas still show signs of minimal fouling to due the MPF "clumps" being highly porous as a result of their irregular stacking (unlike with spherical particles). Connell et al [44] noted a similar phenomenon when examining the filtration of highly branched graphite particles, which were found to have higher flux compared to spherical and platelet particles even at higher particle concentrations.

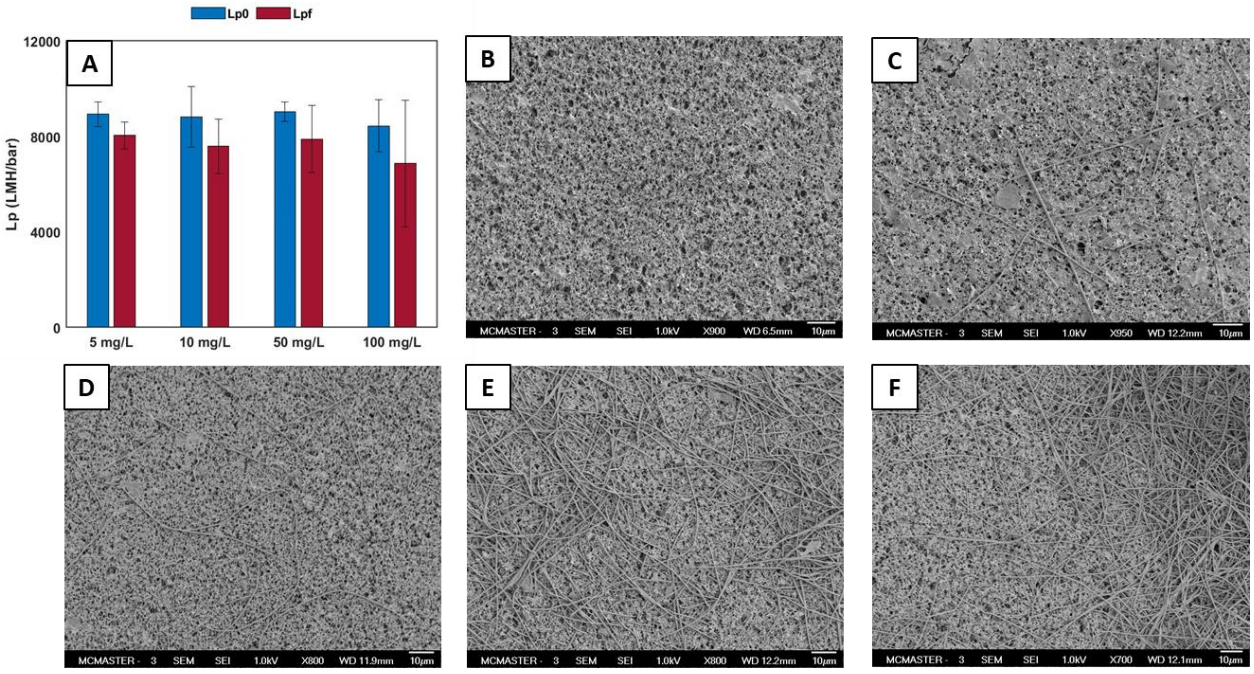

Figure 2.3. Effect of MPF concentration on filtration performance. (A) Membrane permeability measured before (Lp0) and after (Lpf) filtration of MPFs. SEM images of 0.22 um PVDF membrane after filtering 0 mg/L (B), 5mg/L (C), 10 mg/L (D), 50 mg/L (E), and 100 mg/L (F) of MPFs suspended in Milli-Q water.

Figure 2.S2 shows representative permeate and feed optical microscopy images for each concentration studied. Fig. 2.S3a is an image of a permeate sample from the 50 mg/L experiment, indicating complete rejection by the membrane (an observation characteristic of all replicates tested) and consistent with the observed deposition of MPFs on the membrane surface during the experiment (Fig. 2.3). This result is expected as both average dimensions of the MPFs exceed the nominal pore size of the membrane. Lee and Liu [32] found that absolute particle retention occurred for a 0.22 µm PVDF membrane using PS spheres 0.48 µm in diameter, similar to the average diameter of the MPFs. Baltus et al [45] found that orientation is a significant factor in rejection for non-spherical particles, noting that when capsular particles are aligned with the pore they have similar behaviour to spherical particles in terms of rejection when being filtered through track etched membranes. With a PVDF phase inversion membrane, although some pores are larger

than 0.22 µm, MPFs would need to be aligned with the pore opening and pass through the tortuous pore structure to make it into the permeate.

2.3.3 Effect of Membrane Pore Size

The effect of membrane pore size was examined by comparing the filtration of 10 mg/L of MPFs suspended in Milli-Q water through 0.22 µm and 5 µm PVDF membranes. Permeability results displayed in Figure 2.4a show no significant fouling occurring for both the 0.22 µm and 5 µm membranes (Student's t-test on the difference between initial and final permeability had p-values >0.05), while Figure 2.S4 shows corresponding minimal changes in TMP during the 4-hour experiment. SEM images of the 5 µm native membrane and 5 µm membrane following the filtration of a 10 mg/L MPF suspension are shown in Figures 2.4b and c. With the larger pore size membrane (much larger than the diameter and similar to the length of many MPFs), MPFs are observed to both deposit on the membrane surface and enter the membrane pores.

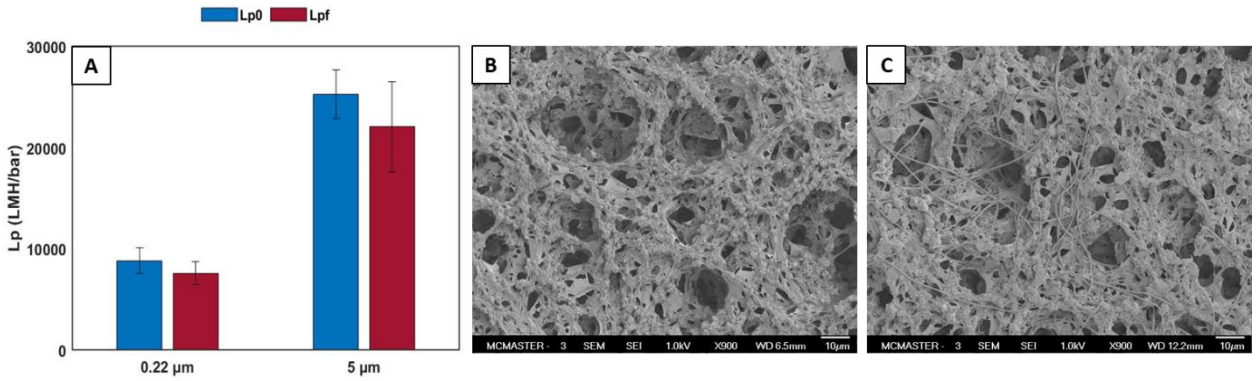

Figure 2.4. Effect of membrane pore size on filtration performance. (A) Membrane permeability measured before (Lp0) and after (Lpf) filtration of 10 mg/L MPFs suspended in Milli-Q water. SEM images of a native 5 µm membrane (B) and 5µm membrane following filtration of the MPF suspension (C).

MPFs were observed in the permeate samples taken from experiments using the 5 µm membrane, as shown in Figure 2.2d. A histogram of the length of MPFs found in the permeate (Figure 2.2c) shows that the majority of MPFs were less than 20 µm in length, smaller than many

of the MPFs present in the feed suspension (Figure 2.2a). Since the MPFs consistently have a smaller diameter than the diameter of the membrane pores, they could enter the pores of the membrane if aligned correctly, although they can be blocked from exiting in the permeate due to the membrane's tortuous pore structure. Shorter MPFs could enter the membrane in more orientations and still permeate through the pores, particularly in light of the observation that some pores in the 5 µm membrane exceed 5 µm (seen in Figure 2.4b). Similar results have been observed in studies investigating the filtration of MPs using MBRs within WWTPs, with the smallest size fraction measured becoming the most abundant in the permeate [29][26][21][20].

2.3.4 Effect of Solution Conditions

To understand the effect of solution conditions, 10 mg/L of MPFs were suspended in secondary clarifier effluent from a municipal WWTP. Figure 2.5 shows the permeability and TMP results for experiments using MPFs suspended in Milli-Q water (MQ), MPFs suspended in secondary clarifier effluent (WW), and WW without MPFs. Filtering MPFs suspended in WW caused a significantly larger drop in permeability and larger TMP rise compared to the filtration of MPFs suspended in Milli-Q water for both the 0.22 and 5 µm membranes. The difference between initial and final permeability was found to be statistically significant for both the 0.22 µm and 5 µm membranes when MPFs were suspended in WW (Student's t-test p-value < 0.05). The change in permeability for the 0.22 µm membrane when filtering WW without MPFs was also statistically significant (p-value <0.05), however the change in permeability for the 5 µm membrane filtering WW alone was not (p-value >0.05). Suspending MPFs in WW led to a greater average TMP rise than WW alone for the 0.22 µm membrane; however, similar TMP profiles were observed for both MPFs suspended in WW and WW without MPFs for the 5 µm membrane (Figure 2.5b and d). The TMP when WW was used had high standard deviations, as shown by the shaded regions in Figure

2.5b and d, due to variation between the individual membranes and WW samples. SEM images of both membranes fouled using WW and MPFs suspended in WW (Figure 2.S5) show significant coverage of the membrane pores for the 0.22 µm membrane. Due to the larger size of the pores in the 5 µm membrane, more of the solids are able to enter the membrane rather than be trapped on the surface, leaving many of the membrane pores still visible upon microscopy analysis. MPFs were not able to be detected in the permeate samples from experiments with WW using optical microscopy (sample feed and permeate images shown in Figure 2.S6) due to the solids in the permeate making any MPFs undistinguishable.

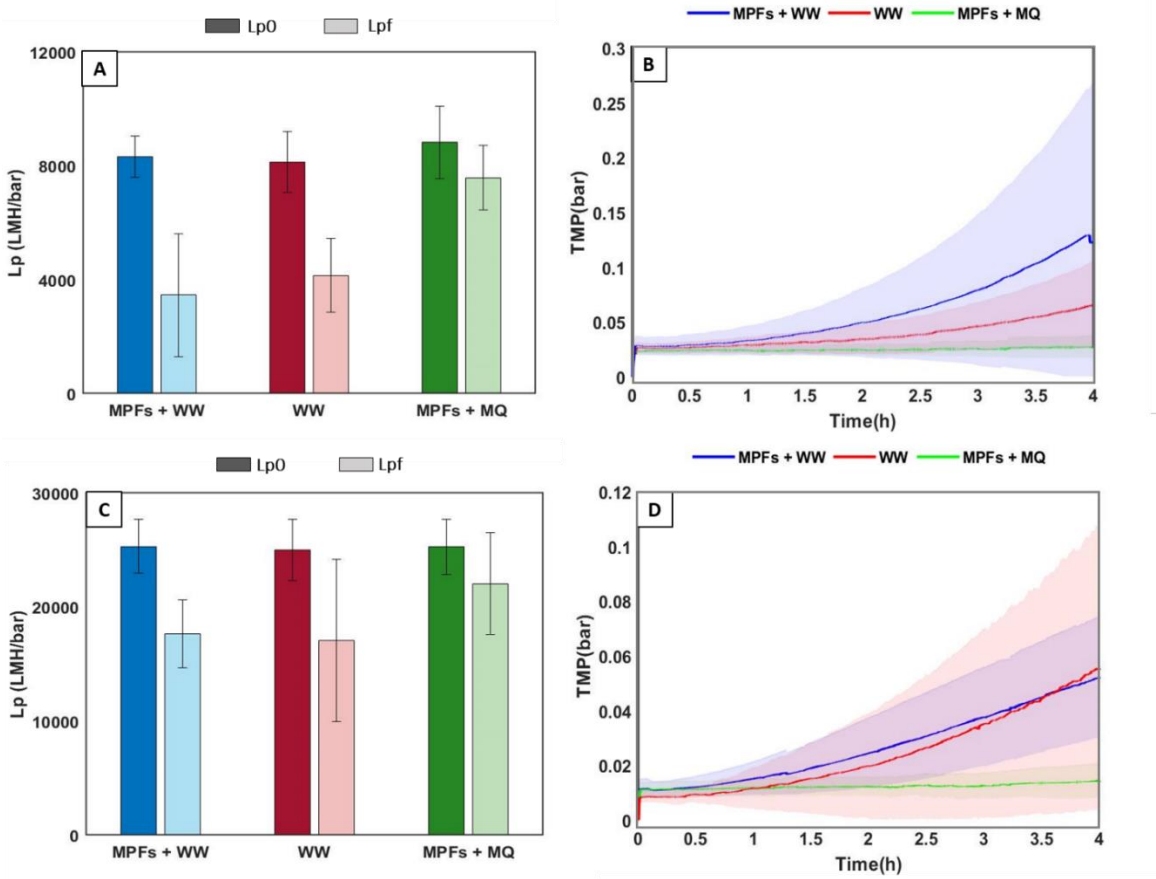

Figure 2.5. Effect of solution conditions on filtration performance. (A) and (C) Membrane permeability before (Lp0) and after (Lpf) a 4-hour filtration of MPFs for the 0.22 µm and 5 µm membranes respectively. (B) and (D) TMP profiles during filtration experiment. Darker colour lines represent TMP averaged over three replicates while the shaded regions represent the standard deviation intervals for the 0.22 µm and 5 µm membranes respectively.

2.4 Discussion

Our observations of the correlation between MPF dimensions and permeability through membranes are consistent with other reported studies on other types of MPs [19][23][24][27][25], with MPFs often observed to have lower removal efficiencies than other particle shapes [18], [23]–[26]. Lares et al [23] noted an increase in the proportion of MPs in the smallest size fraction used in the study (<0.25mm) in MBR permeate, showing that larger MPs are able to be retained by membrane systems. Lv et al [25] reported a similar result, finding that there was an increase in the number of smaller MPs and a decrease in the number of larger MPs across a MBR, attributing the change in size distribution to MP fragmentation. When investigating the filtration of PS and polyamide MP particles using 5 µm cellulose acetate, polycarbonate, and PTFE membranes, Pizzichetti et al [34] also observed the transmission of MPs larger than the nominal membrane pore size, a result attributed to both MP fragmentation (MPs smaller than those in the initial feed were observed in the permeate) and membrane abrasion (MPs 15 times the nominal membrane pore size were found in the permeate). In our work, MPFs are unlikely to cause abrasion like MP particles as they do not have jagged edges; in addition, there were some MPFs in the feed in similar size ranges as those found in the permeate. Therefore, it is unclear if fragmentation is causing more MPFs to exit in the permeate or whether the smaller MPFs are selectively transporting across the membrane. Regardless, both MP fragmentation during filtration and membrane abrasion negatively impact MP removal, with further investigation needed to understand how both of these effects occur and can be prevented.

The fouling effects seen when MPFs are suspended in WW as compared to Milli-Q water, demonstrate the importance of solution conditions in understanding the impacts of MPFs on membrane filtration and fouling. Minimal fouling was observed for both the 0.22 and 5 µm membranes when MPFs are suspended in Milli-Q water but in the presence of WW more

substantial fouling was observed. WW samples can have significant variability both between and within WWTPs, which can affect how MPs interact with the membrane, increasing the importance for using real WW samples in studies. As well, developing better techniques of MP detection is necessary to examine the permeate of more complex feed solutions. There is currently no standard technique for detecting MPs in WW, environmental samples, or laboratory experiments. To better understand the retention of MPFs by the membrane in laboratory experiments, it is crucial to develop either improved detection techniques or MPFs that can be more easily detected.

As the electrospinning process used to create MPFs offers considerable versatility in terms of polymer chemistry, fiber alignment, and fiber diameter, the strategy demonstrated in this work could be tailored to create different types MPFs based on the user's desired properties. Operating parameters such as the applied voltage, feed rate, solution chemistry, needle to collector distance, and collector type can be changed to both optimize the electrospinning process and change the microfiber morphology. For instance, increasing the applied voltage, increasing polymer feed rate, decreasing solution conductivity, increasing polymer concentration, and decreasing the distance between the needle tip and collector have been found to increase fiber diameter [46][47]. This process allows fibers to be created using a variety of polymers that are representative of common MPF chemistries such as nylon [48], polyethylene terephthalate [49], and polypropylene [50] as well as polymers more commonly used in biomedical applications [43][44][48]. By combining electrospinning with the cryostat cutting technique developed by Cole [38], MPFs with different properties can be created to better understand their impacts on the environment and mitigate their release.

2.5 Conclusions

PS MPFs averaging 73 µm in length and 0.52 µm in diameter were fabricated by combining electrospinning with a cryostat cutting procedure. The MPFs were used in filtration experiments to examine their impacts on membrane filtration with respect to feed concentration, membrane pore size, and solution conditions. When suspended in Milli-Q water, MPFs did not significantly contribute to membrane fouling at any tested concentrations as the MPFs formed a highly porous cake when depositing on the membrane; correspondingly, MPFs were observed in permeate samples when filtered through a 5 µm membrane, although the permeated MPFs were much smaller than the average length in the feed as the longer MPFs were caught in the pore structure of the membrane. The importance of using solution conditions representative of those found in WWTPs was shown as MPFs suspended in secondary clarifier water from a municipal WWTP increased the fouling effects seen on both the 0.22 µm and 5 µm pore size membranes.

This work represents an initial investigation into how MPFs impact membrane filtration. As membrane systems in WWTPs have shown to be more (but not absolutely) effective than other unit operations for MP removal, it is imperative to understand the effects MPs of all shapes, sizes, and chemistries may have on the system. Understanding the impact of both MP and membrane properties on membrane filtration and fouling in WWTPs will allow for the improved design and operation of filtration systems, enabling reductions in the discharge of MPs into the environment.

2.6 References

[1] D. Eerkes-Medrano, R. C. Thompson, and D. C. Aldridge, “Microplastics in freshwater systems: A review of the emerging threats, identification of knowledge gaps and prioritisation of research needs,” *Water Res.*, vol. 75, pp. 63–82, 2015, doi: 10.1016/j.watres.2015.02.012.

[2] A. L. Andrady, “Microplastics in the marine environment,” *Mar. Pollut. Bull.*, vol. 62, no. 8, pp. 1596–1605, 2011, doi: 10.1016/j.marpolbul.2011.05.030.

[3] M. Cole, P. Lindeque, C. Halsband, and T. S. Galloway, “Microplastics as contaminants in the marine environment: A review,” *Mar. Pollut. Bull.*, vol. 62, no. 12, pp. 2588–2597,

2011, doi: 10.1016/j.marpolbul.2011.09.025.

[4] J. Gago, O. Carretero, A. V. Filgueiras, and L. Viñas, “Synthetic microfibers in the marine environment: A review on their occurrence in seawater and sediments,” *Mar. Pollut. Bull.*, vol. 127, no. July 2017, pp. 365–376, 2018, doi: 10.1016/j.marpolbul.2017.11.070.

[5] World Health Organization, “Microplastics in Drinking Water,” Geneva, 2019. [Online]. Available: http://library1.nida.ac.th/termpaper6/sd/2554/19755.pdf.

[6] R. Dris, J. Gasperi, M. Saad, C. Mirande, and B. Tassin, “Synthetic fibers in atmospheric fallout: A source of microplastics in the environment?,” *Mar. Pollut. Bull.*, vol. 104, no. 1–2, pp. 290–293, 2016, doi: 10.1016/j.marpolbul.2016.01.006.

[7] J. Sun, X. Dai, Q. Wang, M. C. M. van Loosdrecht, and B. J. Ni, “Microplastics in wastewater treatment plants: Detection, occurrence and removal,” *Water Res.*, vol. 152, pp. 21–37, 2019, doi: 10.1016/j.watres.2018.12.050.

[8] A. Bakir, S. J. Rowland, and R. C. Thompson, “Enhanced desorption of persistent organic pollutants from microplastics under simulated physiological conditions,” *Environ. Pollut.*, vol. 185, pp. 16–23, 2014, doi: 10.1016/j.envpol.2013.10.007.

[9] Y. Chae and Y. J. An, “Effects of micro- and nanoplastics on aquatic ecosystems: Current research trends and perspectives,” *Mar. Pollut. Bull.*, vol. 124, no. 2, pp. 624–632, 2017, doi: 10.1016/j.marpolbul.2017.01.070.

[10] B. Ma, W. Xue, C. Hu, H. Liu, J. Qu, and L. Li, “Characteristics of microplastic removal via coagulation and ultrafiltration during drinking water treatment,” *Chem. Eng. J.*, vol. 359, no. November 2018, pp. 159–167, 2019, doi: 10.1016/j.cej.2018.11.155.

[11] D. D. A. Miranda and G. F. De Carvalho-souza, “Are we eating plastic-ingesting fi sh ?,” *Mar. Pollut. Bull.*, vol. 103, no. 1–2, pp. 109–114, 2016, doi: 10.1016/j.marpolbul.2015.12.035.

[12] J. C. Prata, “Microplastics in wastewater: State of the knowledge on sources, fate and solutions,” *Mar. Pollut. Bull.*, vol. 129, no. 1, pp. 262–265, 2018, doi: 10.1016/j.marpolbul.2018.02.046.

[13] M. A. Browne *et al.*, “Accumulation of microplastic on shorelines woldwide: Sources and sinks,” *Environ. Sci. Technol.*, vol. 45, no. 21, pp. 9175–9179, 2011, doi: 10.1021/es201811s.

[14] M. Enfrin, L. F. Dumée, and J. Lee, “Nano/microplastics in water and wastewater treatment processes – Origin, impact and potential solutions,” *Water Res.*, vol. 161, pp. 621–638, 2019, doi: 10.1016/j.watres.2019.06.049.

[15] T. Poerio, E. Piacentini, and R. Mazzei, “Membrane processes for microplastic removal,” *Molecules*, vol. 24, no. 22, 2019, doi: 10.3390/molecules24224148.

[16] H. A. Leslie, S. H. Brandsma, M. J. M. van Velzen, and A. D. Vethaak, “Microplastics en route: Field measurements in the Dutch river delta and Amsterdam canals, wastewater treatment plants, North Sea sediments and biota,” *Environ. Int.*, vol. 101, pp. 133–142, 2017, doi: 10.1016/j.envint.2017.01.018.

[17] M. Simon, A. Vianello, and J. Vollertsen, “Removal of > 10 μm microplastic particles from treated wastewater by a disc filter,” *Water (Switzerland)*, vol. 11, no. 9, 2019, doi: 10.3390/w11091935.

[18] M. R. Michielssen, E. R. Michielssen, J. Ni, and M. B. Duhaime, “Fate of microplastics and other small anthropogenic litter (SAL) in wastewater treatment plants depends on unit processes employed,” *Environ. Sci. Water Res. Technol.*, vol. 2, no. 6, pp. 1064–1073, 2016, doi: 10.1039/c6ew00207b.

[19] L. Li, D. Liu, K. Song, and Y. Zhou, “Performance evaluation of MBR in treating microplastics polyvinylchloride contaminated polluted surface water,” *Mar. Pollut. Bull.*, vol. 150, no. November 2019, pp. 1–6, 2020, doi: 10.1016/j.marpolbul.2019.110724.

[20] C. Baresel *et al.*, “Membrane Bioreactor Processes to Meet Todays and Future Municipal Sewage Treatment Requirements?,” *Int. J. Water Wastewater Treat.*, vol. 3, no. 2, 2017, doi: 10.16966/2381-5299.140.

[21] C. Baresel, M. Harding, and J. Fang, “Ultrafiltration/granulated active carbon-biofilter: Efficient removal of a broad range of micropollutants,” *Appl. Sci.*, vol. 9, no. 4, 2019, doi: 10.3390/app9040710.

[22] J. Bayo, J. López-Castellanos, and S. Olmos, “Membrane bioreactor and rapid sand filtration for the removal of microplastics in an urban wastewater treatment plant,” *Mar. Pollut. Bull.*, vol. 156, no. March, p. 111211, 2020, doi: 10.1016/j.marpolbul.2020.111211.

[23] M. Lares, M. C. Ncibi, M. Sillanpää, and M. Sillanpää, “Occurrence, identification and removal of microplastic particles and fibers in conventional activated sludge process and advanced MBR technology,” *Water Res.*, vol. 133, pp. 236–246, 2018, doi: 10.1016/j.watres.2018.01.049.

[24] H. Hidayaturrahman and T. G. Lee, “A study on characteristics of microplastic in wastewater of South Korea: Identification, quantification, and fate of microplastics during treatment process,” *Mar. Pollut. Bull.*, vol. 146, no. July, pp. 696–702, 2019, doi: 10.1016/j.marpolbul.2019.06.071.

[25] X. Lv, Q. Dong, Z. Zuo, Y. Liu, X. Huang, and W. M. Wu, “Microplastics in a municipal wastewater treatment plant: Fate, dynamic distribution, removal efficiencies, and control strategies,” *J. Clean. Prod.*, vol. 225, pp. 579–586, 2019, doi: 10.1016/j.jclepro.2019.03.321.

[26] S. Ziajahromi, P. A. Neale, L. Rintoul, and F. D. L. Leusch, “Wastewater treatment plants as a pathway for microplastics: Development of a new approach to sample wastewater-based microplastics,” *Water Res.*, vol. 112, pp. 93–99, 2017, doi: 10.1016/j.watres.2017.01.042.

[27] S. Olmos, J. López-Castellanos, and J. Bayo, “Are advanced wastewater treatment technologies a solution for total removal of microplastics in treated effluents?,” *WIT Trans. Ecol. Environ.*, vol. 229, pp. 109–116, 2019, doi: 10.2495/WRM190111.

[28] A. Foglia *et al.*, “Anaerobic membrane bioreactor for urban wastewater valorisation:

Operative strategies and fertigation reuse," *Chem. Eng. Trans.*, vol. 74, no. November 2018, pp. 247–252, 2019, doi: 10.3303/CET1974042.

[29] J. Talvitie, A. Mikola, A. Koistinen, and O. Setälä, "Solutions to microplastic pollution – Removal of microplastics from wastewater effluent with advanced wastewater treatment technologies," *Water Res.*, vol. 123, pp. 401–407, 2017, doi: 10.1016/j.watres.2017.07.005.

[30] H. Lee, D. Segets, S. Süß, W. Peukert, S. C. Chen, and D. Y. H. Pui, "Liquid filtration of nanoparticles through track-etched membrane filters under unfavorable and different ionic strength conditions: Experiments and modeling," *J. Memb. Sci.*, vol. 524, no. August 2016, pp. 682–690, 2017, doi: 10.1016/j.memsci.2016.11.023.

[31] D. Breite, M. Went, I. Thomas, A. Prager, and A. Schulze, "Particle adsorption on a polyether sulfone membrane: How electrostatic interactions dominate membrane fouling," *RSC Adv.*, vol. 6, no. 70, pp. 65383–65391, 2016, doi: 10.1039/c6ra13787c.

[32] J. K. Lee and B. Y. H. Liu, "An experimental study of particulate retention by microporous membranes in liquid filtration," *KSME J.*, vol. 8, no. 1, pp. 69–77, 1994, doi: 10.1007/BF02953245.

[33] M. Enfrin, J. Lee, P. Le-Clech, and L. F. Dumée, "Kinetic and mechanistic aspects of ultrafiltration membrane fouling by nano- and microplastics," *J. Memb. Sci.*, vol. 601, no. January, 2020, doi: 10.1016/j.memsci.2020.117890.

[34] A. R. P. Pizzichetti, C. Pablos, C. Álvarez-Fernández, K. Reynolds, S. Stanley, and J. Marugán, "Evaluation of membranes performance for microplastic removal in a simple and low-cost filtration system," *Case Stud. Chem. Environ. Eng.*, vol. 3, no. December 2020, p. 100075, 2021, doi: 10.1016/j.cscee.2020.100075.

[35] B. Agasanapura, R. E. Baltus, C. T. Tanneru, and S. Chellam, "Effect of electrostatic interactions on rejection of capsular and spherical particles from porous membranes: Theory and experiment," *J. Colloid Interface Sci.*, vol. 448, pp. 492–500, 2015, doi: 10.1016/j.jcis.2015.02.016.

[36] A. Delavari, B. Agasanapura, and R. E. Baltus, "The effect of particle rotation on the motion and rejection of capsular particles in slit pores," *AIChE J.*, vol. 64, no. 7, pp. 2828–2836, 2018, doi: 10.1002/aic.16132.

[37] F. De Falco, E. Di Pace, M. Cocca, and M. Avella, "The contribution of washing processes of synthetic clothes to microplastic pollution," *Sci. Rep.*, no. January, pp. 1–11, 2019, doi: 10.1038/s41598-019-43023-x.

[38] M. Cole, "A novel method for preparing microplastic fibers," *Sci. Rep.*, vol. 6, no. October, pp. 1–7, 2016, doi: 10.1038/srep34519.

[39] M. W. Lee, S. An, S. S. Latthe, C. Lee, S. Hong, and S. S. Yoon, "Electrospun Polystyrene Nanofiber Membrane with Superhydrophobicity and Superoleophilicity for Selective Separation of Water and Low Viscous Oil," *Appl. Mater. Interfaces*, 2013, doi: 10.1021/am404156k.

[40] T. Jarusuwannapoom and W. Hongrojjanawiwat, “Effect of solvents on electro-spinnability of polystyrene solutions and morphological appearance of resulting electrospun polystyrene fibers,” *Eurpoean Polym. J.*, vol. 41, pp. 409–421, 2005, doi: 10.1016/j.eurpolymj.2004.10.010.

[41] M. Zhou, H. Liu, J. E. Kilduff, R. Langer, D. G. Anderson, and G. Belfort, “High Throughput Synthesis and Screening of New Protein Resistant Surfaces for Membrane Filtration,” *AIChE J.*, vol. 56, no. 7, pp. 1932–1945, 2010, doi: 10.1002/aic.12104.

[42] H. Choi, K. Zhang, D. D. Dionysiou, D. B. Oerther, and G. A. Sorial, “Effect of permeate flux and tangential flow on membrane fouling for wastewater treatment,” *Sep. Purif. Technol.*, vol. 45, no. 1, pp. 68–78, 2005, doi: 10.1016/j.seppur.2005.02.010.

[43] M. Simon, N. van Alst, and J. Vollertsen, “Quantification of microplastic mass and removal rates at wastewater treatment plants applying Focal Plane Array (FPA)-based Fourier Transform Infrared (FT-IR) imaging,” *Water Res.*, vol. 142, pp. 1–9, 2018, doi: 10.1016/j.watres.2018.05.019.

[44] H. Connell, J. Zhu, and A. Bassi, “Effect of particle shape on crossflow filtration flux,” *J. Memb. Sci.*, vol. 153, no. February 1998, 1999.

[45] R. E. Baltus, A. R. Badireddy, W. Xu, and S. Chellam, “Analysis of configurational effects on hindered convection of nonspherical bacteria and viruses across microfiltration membranes,” *Ind. Eng. Chem. Res.*, vol. 48, no. 5, pp. 2404–2413, 2009, doi: 10.1021/ie800579e.

[46] A. Haider, S. Haider, and I. K. Kang, “A comprehensive review summarizing the effect of electrospinning parameters and potential applications of nanofibers in biomedical and biotechnology,” *Arab. J. Chem.*, vol. 11, no. 8, pp. 1165–1188, 2018, doi: 10.1016/j.arabjc.2015.11.015.

[47] A. Greiner and J. H. Wendorff, “Electrospinning: A fascinating method for the preparation of ultrathin fibers,” *Angew. Chemie - Int. Ed.*, vol. 46, no. 30, pp. 5670–5703, 2007, doi: 10.1002/anie.200604646.

[48] H. Fong, W. Liu, C. S. Wang, and R. A. Vaia, “Generation of electrospun fibers of nylon 6 and nylon 6-montmorillonite nanocomposite,” *Polymer (Guildf).*, vol. 43, no. 3, pp. 775–780, 2001, doi: 10.1016/S0032-3861(01)00665-6.

[49] Z. Ma, M. Kotaki, T. Yong, W. He, and S. Ramakrishna, “Surface engineering of electrospun polyethylene terephthalate (PET) nanofibers towards development of a new material for blood vessel engineering,” *Biomaterials*, vol. 26, no. 15, pp. 2527–2536, 2005, doi: 10.1016/j.biomaterials.2004.07.026.

[50] K. H. Lee *et al.*, “Electrospinning of syndiotactic polypropylene from a polymer solution at ambient temperatures,” *Macromolecules*, vol. 42, no. 14, pp. 5215–5218, 2009, doi: 10.1021/ma9006472.

[51] N. Bhardwaj and S. C. Kundu, “Electrospinning: A fascinating fiber fabrication technique,” *Biotechnol. Adv.*, vol. 28, no. 3, pp. 325–347, 2010, doi: 10.1016/j.biotechadv.2010.01.004.

2.7 Supplemental Information

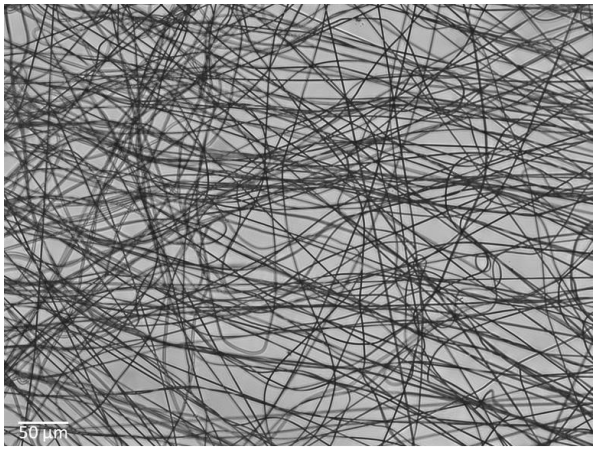

Figure 2.S1. Electrospun fiber mat prior to freezing and cutting.

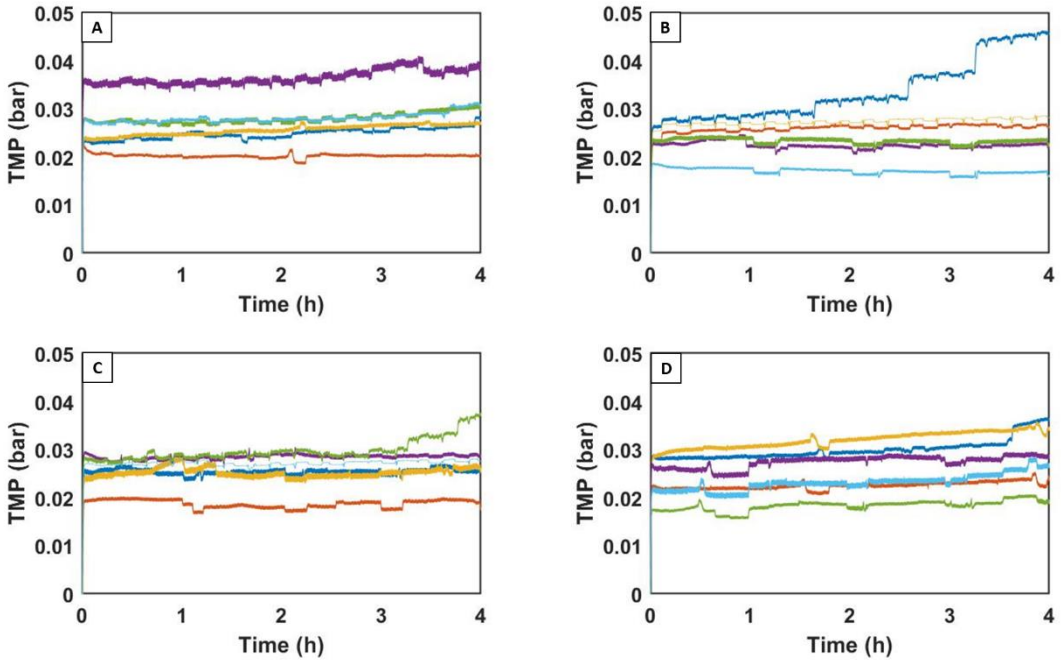

Figure 2.S2. TMP profiles for the 5 mg/L (A), 10 mg/L (B), 50 mg/L (C), and 100 mg/L (D) MPF experiments suspended in Milli-Q water using 0.22 µm PVDF membranes.

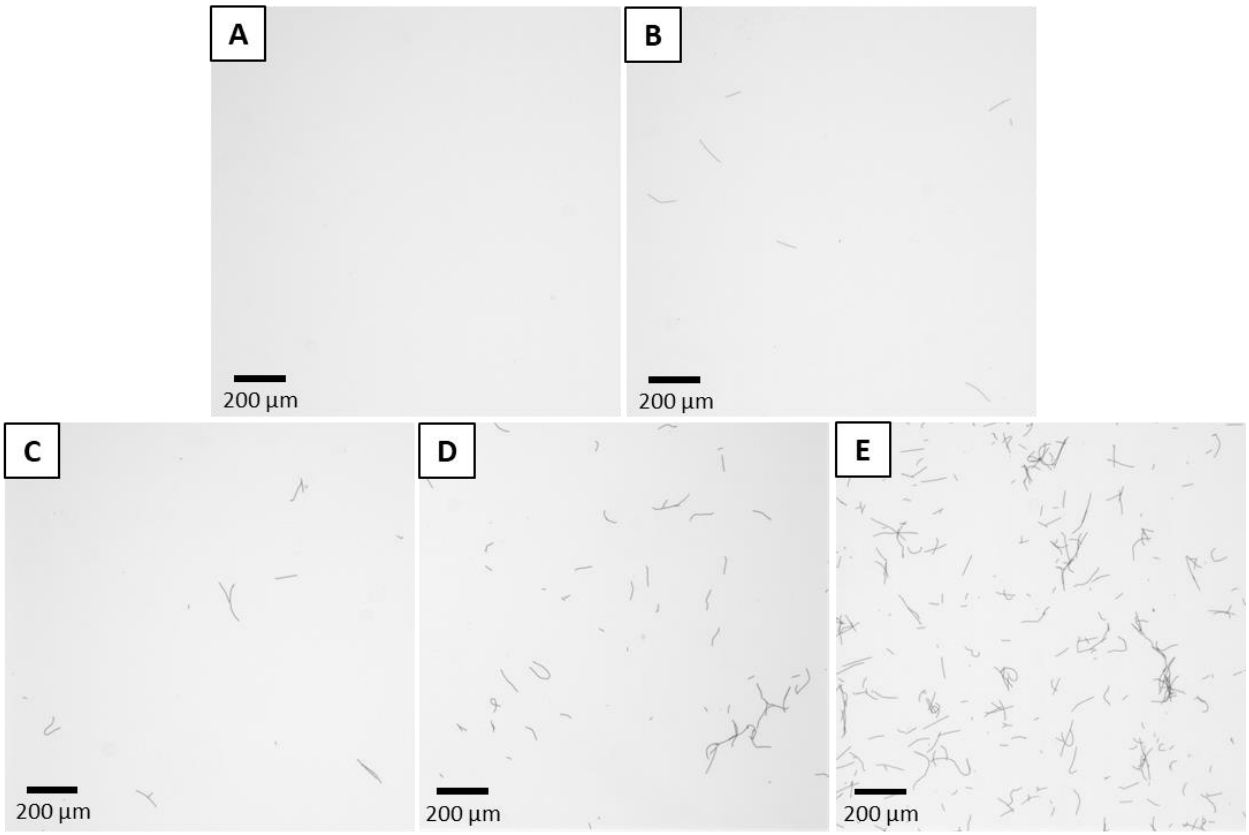

Figure 2.S3. Optical microscope images of (A) a permeate sample from filtering 50 mg/L and (B)-(E) feed samples from 5, 10, 50, and 100 mg/L of MPFs were suspended in Milli-Q water and filtered through 0.22 µm membranes. (A) is representative of what was found in all permeate samples for all experiments using 0.22 µm membranes.

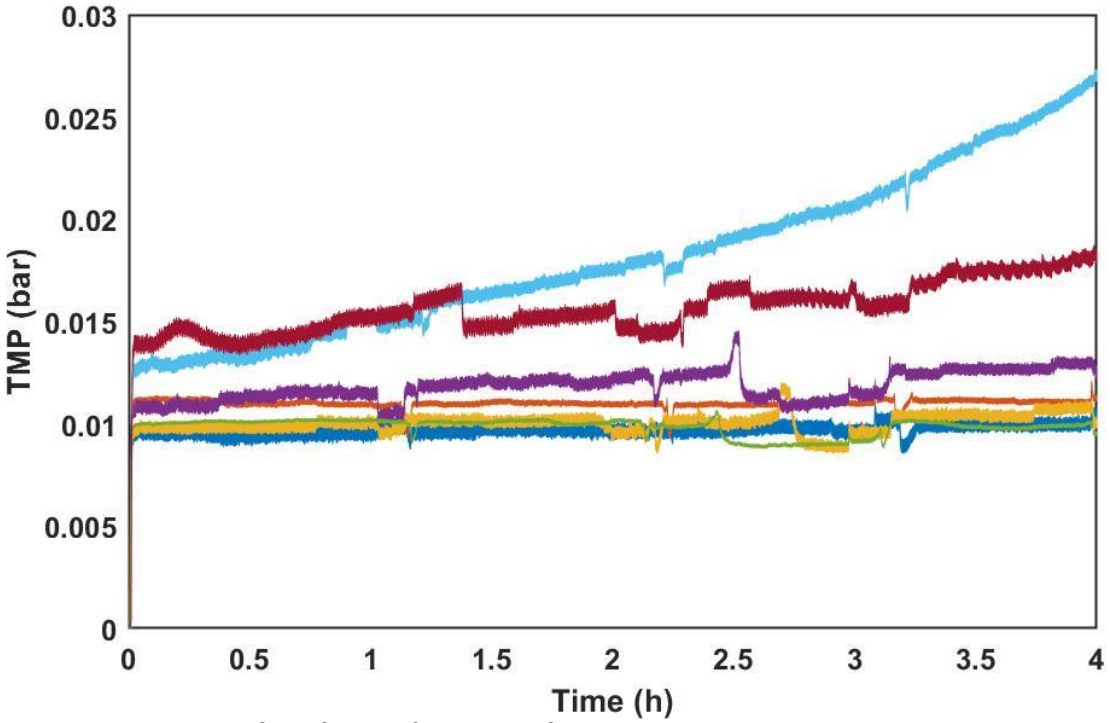

Figure 2.S4. TMP profiles for the filtration of 10 mg/L MPFs suspended in Milli-Q water through 5 µm PVDF membranes.

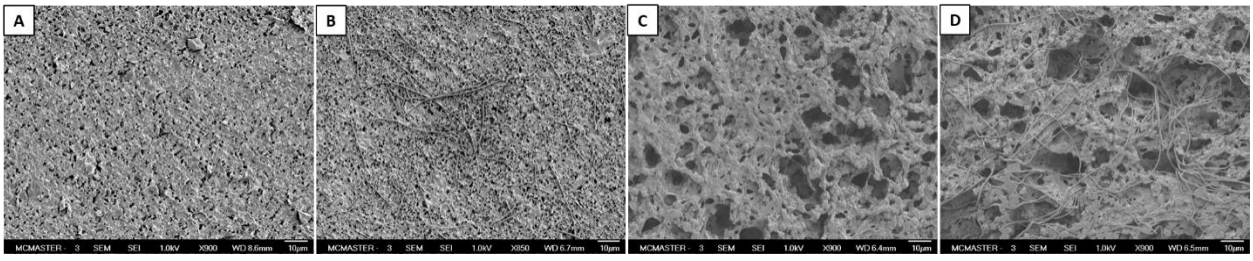

Figure 2.S5. SEM images of 0.22 µm membranes after the filtration of WW (A) and MPFs suspended in WW (B) and 5 µm membranes after the filtration of WW (C) and MPFs suspended in WW (D).

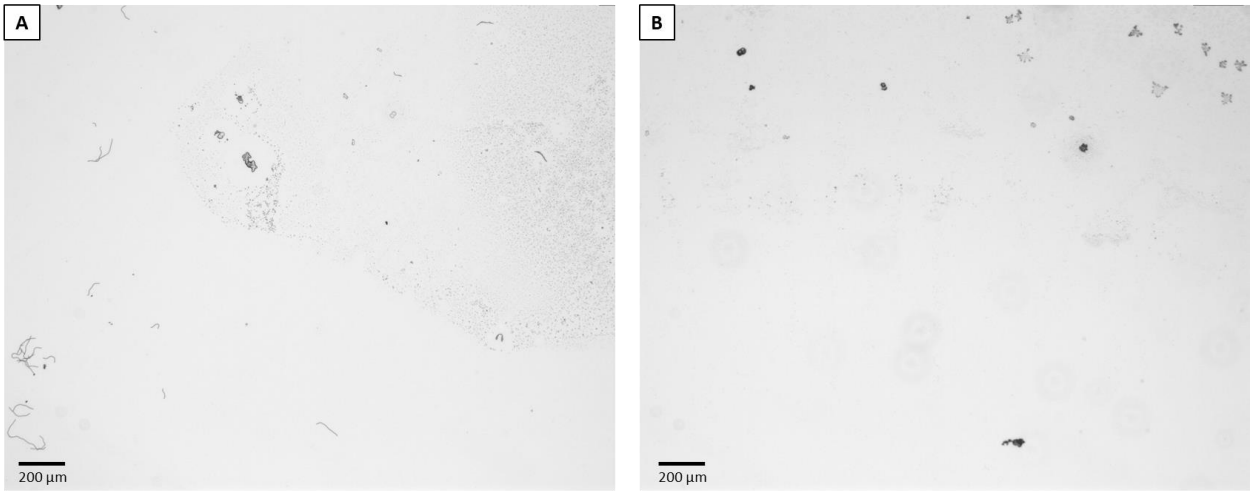

Figure 2.S6. Optical microscope images of (A) feed sample and (B) permeate sample from filtering 10 mg/L of MPFs suspended in WW through 5 µm membranes.

Chapter 3: Understanding the impact of fiber length on membrane filtration using fluorescent microplastic fibers

3.1 Introduction

The increased production and use of plastic items has lead to widespread contamination of microplastics (MPs) in freshwater and marine environments [1][2]. MPs have been found to vary significantly in terms of their size (ranging from 1 μm to 5 mm) and shape (fragments, fibers, films, microbeads, etc), rendering them difficult to detect and remove [3]. Wastewater treatment plants (WWTPs) have been found to be a significant source of MPs into the environment as they can discharge up to 10^{10} MPs per day [4]. Membrane filtration systems used in some WWTPS, often in the form of membrane bioreactors (MBRs) or as tertiary treatment steps, are a promising removal technology as the size of membrane pores (0.002 – 10 μm) are often smaller than majority of MPs. Membrane filtration has been shown to be just as or more effective in the removal of MPs as compared to other polishing steps in WWTPs such as disc filters, rapid sand filtration, and dissolved air filtration, removing 79-99.9% of MPs [5][6][7][8][9].

Though membrane filtration is effective at removing majority of MPs, removal efficiency can vary based on MP properties. MP fibers (MPFs) have been found to have lower removal efficiencies compared to MP particles, with removal efficiencies of 98.83% and 57.65% being reported for MP particles as compared to MPFs [6]. This lower removal efficiency is of concern as MPFs have been found to represent up to 60% of MPs observed in WWTP influents [10][6][11], being generated from the laundering of synthetic textiles [12]. Studies within WWTPs have investigated the removal of MPs using membrane systems but are not able to provide significant details on the interactions between MPs and membrane systems. There have been several studies, all published within the last two years, that have investigated the effects of MPs on membrane filtration. In these studies, MPs were found to cause significant membrane fouling during filtration

[13][14][15]. As well, Pizzichetti et al. [14] found MPs in the permeate of a 5 µm that exceeded the nominal membrane pore size. These studies provide insight into the effects of MPs on membrane filtration but they are limited to MP fragments/particles. With MPFs being prevalent in WWTPs, it is critical to understand how they impact membrane filtration.

Our previous work in the previous chapter found that MPFs were present in the permeate of 5 µm membranes, with some having lengths larger than the nominal membrane pore size. With MPs in WWTPs varying significantly in size, it is key to understand how length may impact MPF rejection. The smallest size fraction of MPs measured has been found to be more abundant in the permeate as compared to feed samples in works investigating MP filtration in WWTPs [5][16][17][18]. The proportion of small MPs exiting in the membrane permeate may be higher than reported as often MPs less than 10 µm are not able to be detected. Studies that measured MPs 1-10 µm in size have reported significantly higher concentrations of MPs compared to studies that could only measure MPs greater than 10 µm [19]. WWTPs have the potential to cause fragmentation of MPs during treatment, resulting in smaller MPs than those in the original influent [20]. With the discovery of NPs in marine environments, it is critical to understand how MP size may impact particle rejection [21]. As well, in the previous chapter MPFs were detect by optical microscopy alone. This method was not the most effective to understand MPF concentration in the permeate and was unable to detect MPFs suspended in WW. Developing MPFs that can be easily detected in samples from filtration experiments would allow for a better understanding of MPF filtration.

In this work, fluorescent polystyrene MPFs that can be detected visually using fluorescent microscopy and in suspension were created. The fluorescent MPFs were made with two different length distributions to analyze the impact of length on MPF transmission. Filtration experiments

using both lengths of MPFs were performed using 5 µm and 0.22 µm PVDF membranes to understand the impact of length relating to membrane pore size.

3.2 Materials and Methods

3.2.1 Microplastic Fiber Synthesis

Polystyrene (PS, M_w ~192000 g/mol), N,N,dimethylformamide (DMF), and meso-tetraphenylporphyrin (TPP) were purchased from Sigma Aldrich. The chemical structure and excitation and emission spectra for TPP are shown in Figure 3.1. PS and TPP were dissolved in DMF to create a 30 wt% polymer solution with 2 mg/mL of TPP based on work by Hu et al [22]. A 1 mL syringe with a 25-gauge needle was filled with the fluorescent PS solution and loaded into a syringe pump which extruded the solution at a rate of 2 µL/min. A high voltage power supply was used to apply a voltage of 15 kV between the needle and rotating drum collector (3 cm in diameter) to electrospin the polymer solution into a fiber mat. The electrospun fibers were collected on a piece of aluminum foil attached to the collector, which rotated at a speed of 2000 rpm. The distance between the needle and the collector was 5 cm. Images of the electrospun mats are shown in Figure 3.S1. The electrospun fiber mat was cut into MPFs using a cryostat cutting protocol adapted from Cole [23]. The fiber mat was coated in freezing compound (Tissue-Tek) and frozen for at least 20 minutes in a -20^{o}C freezer. The frozen fiber mat was then cut into sections and frozen together into a block to fit onto the cryostat chuck using the freezing compound. The block was then cut at lengths of 20 µm and 100 µm using a cryostat (Leica CM3050) to create two MPF samples, c20 and c100, for use in filtration experiments. The cut MPFs were placed in a glass vials filled with room temperature Milli-Q water and mixed using a magnetic stir bar overnight to thaw and separate the MPFs. The freezing compound was removed by filtering the MPF solution through an Ahlstrom-Munksjö 610 filter paper and gently collecting the MPFs retained off of the top of the filter paper. Purified MPFs were suspended in Milli-Q water and sonicated for 30

minutes using an ultrasonic bath (Branson). To prepare MPF suspensions for filtration experiments, the MPF stock suspension was diluted to a volume of 160 mL in Milli-Q water to achieve an MPF concentration of 10 mg/L. The suspension was vortexed to ensure even dispersion and sonicated in an ultrasonic bath for 1 hour to ensure disaggregation. Prior to use in filtration experiments, MPFs were kept in the dark to prevent photobleaching.

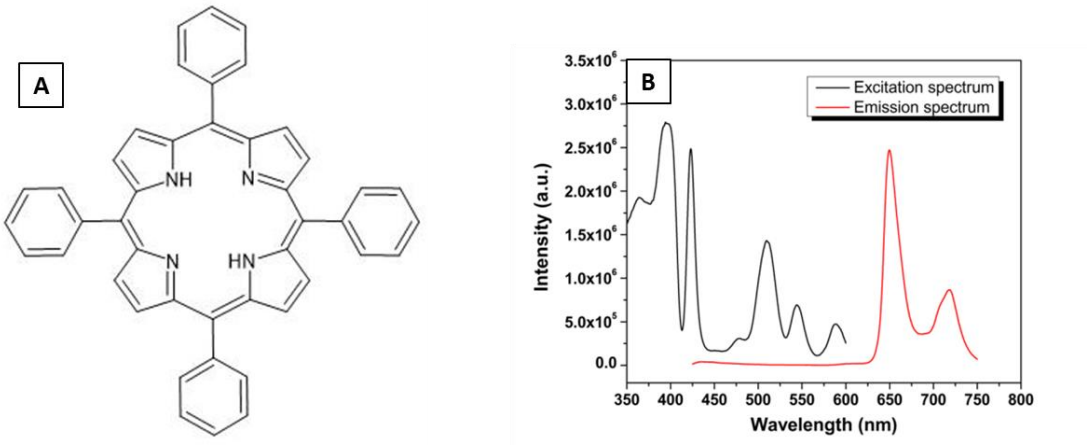

Figure 3.1. Chemical structure (A) and excitation and emission spectras (B) of TPP. Excitation and emission spectra adapted from [24].

3.2.2 Filtration Experiments

PVDF Durapore membranes with nominal pore size of 0.22 µm (purchased from Sigma Aldrich) and 5 µm (donated by Millipore) were used in filtration experiments. A custom filtration set up (shown in Figure 2.1) consisting of a multi-channel peristaltic pump connected to an acetal (polyoxymethylene copolymer) block fitted with three separate channels that housed individual membrane holders (Cole-Parmer) was used to conduct three filtration experiments in parallel. Transmembrane pressure (TMP) was monitored throughout the experiments for each membrane using three USB pressure transducers (Omega PX409) screwed into the acetal (polyoxymethylene copolymer) block.

Prior to conducting filtration experiments, the membranes were placed inside of the membrane holders and the membranes were wet by passing 20 mL of Milli-Q water through each membrane. The membrane holders were then attached to the filtration set up and Milli-Q water was passed through the membranes at 450 $L/m^2/h$ (LMH) for 10 minutes or until constant TMP was reached. Hydraulic permeability (L_p) was measured before the filtration of MPFs using six flux values between 120 – 360 LMH, repeating each flux twice. The true permeate flux was measured by collecting permeate in a 48 well plate for each membrane and determining the volume collected over time by measuring absorbance at 977 nm using a plate reader (Tecan) [25].

Following the initial permeability measurement, the membranes were used to filter a suspension of MPFs for a duration of 4 hours at 225 ± 40 LMH (where the ± represents standard deviation). The true permeate flux during the filtration experiment was measured due to variation between different pump channels. TMP was logged continuously during MPF filtration and 1 mL permeate samples were collected every 30 minutes. After MPF filtration, the membrane holders were removed from the set-up and the solution on top of the membrane was removed using a pipette. The filtration set-up was rinsed thoroughly with Milli-Q water before reattaching the membrane holders. A second permeability measurement was then taken using the same process as described for the initial permeability. Following the final permeability measurement, the membranes were carefully removed from the membrane holders to be used for microscopy analysis.

Following each filtration experiment, a 150 µL aliquot of each permeate and feed sample was transferred to a black half area 96-well plate (Perkin Elmer). The fluorescence intensity of each sample was measured using an Infinite M1000 Plate Reader (Tecan) at excitation and emission wavelengths of 420 nm and 651 nm, based on the supplier's recommendations. The

fluorescent intensity of the c20 MPFs was measured at a gain of 190 and 20 nm bandwidth for the excitation and emission wavelengths. The fluorescent intensity of the c100 MPFs was measured at a gain of 255 and 10 nm bandwidth for the excitation and emission wavelengths. Calibration curves for each length of MPF used were created by measuring the fluorescent intensity of known concentrations of MPF samples, shown in Figure 3.2a.

3.2.3 Microscopy Analysis

Electropun fiber mats and MPFs were imaged using an Olympus inverted IX51 microscope with a QImaging Retiga 2000R camera. For feed and permeate samples from filtration experiment, 20 µL of sample was pipetted into a 48 well plate and dried in an over at 60^{o}C. Brightfield and fluorescent images were taken of each sample. Fluorescent images were taken using a filter with excitation and emission wavelengths of 448 nm and 623 nm respectively. ImageJ Analysis Software was used to determine the length, diameter, and concentration of the MPFs.

The membrane surface was imaged following filtration experiments using a JEOL 7000F field-emission scanning electron microscope (SEM). The membranes were allowed to completely dry at room temperature prior to being mounted on an aluminum SEM stub and sputter coated with a 5 nm platinum coating. The membranes were imaged using a 1 kV acceleration voltage.

3.3 Results and Discussion

3.3.1 Microplastic Fiber Fluorescence

MPFs were made fluorescent by doping the electrospinning solution with 2 mg/mL of TPP. MPF fluorescence allowed for MPFs to be detected using fluorescence microscopy, as shown in Figure 3.2b and c, as well as in suspension. Figure 3.2a shows calibration curves relating fluorescent intensity to concentration for c20 and c100 MPFs suspended in Milli-Q water. A linear

relationship was found to be a good fit to describe the relationship between fluorescent intensity and concentration, both c20 and c100 MPFs having R^2 values exceeding 0.97. The approach of doping the electrospinning solution with a fluorophore was taken as fluorescent electrospinning has been shown to yield good results for other applications such as chemical detection [26][22], photodynamic inactivation of bacteria [27], and optoelectronic devices [28]. Two different fluorophores, fluorescein and anthracene, were tested prior to using TPP; TPP being found to be the most effective. Fluorescein was found to leach from the MPFs, resulting in inaccurate fluorescent intensity measurements. Anthracene is insoluble in water, making it unlikely to leach from the MPFs, but did not produce fluorescent intensity measurements that could be differentiated based on MPF concentration. Fluorescent intensity data for MPFs doped with fluorescein and anthracene are shown in Figures 3.S2 and 3.S3. TPP is insoluble in water and therefore unlikely leach from the MPFs [29]. It also produces fluorescent intensity values that can relate to MPF concentration, making it the most effective fluorophore based on those tested. Higher concentrations of TPP were tested (5 mg/mL and 10 mg/mL) in an effort to increase the detection sensitivity of the MPFs but these concentrations produced polymer solutions that were very difficult to electrospin into fibers.

The creation of MPFs that can be easily detected is crucial for the detailed understanding of the interactions between MPFs and membranes. Enabling the detection of MPFs within the membrane as well as in feed and permeate samples allows for other variables in the filtration process to be studied such as properties of the MPFs or process such as membrane type, solution chemistry, and operating parameters. Fluorescent MPFs also could allow for them to be detected in more complex solutions such as WW, where in the previous chapter MPFs suspended in WW could not be detected using optical microscopy.

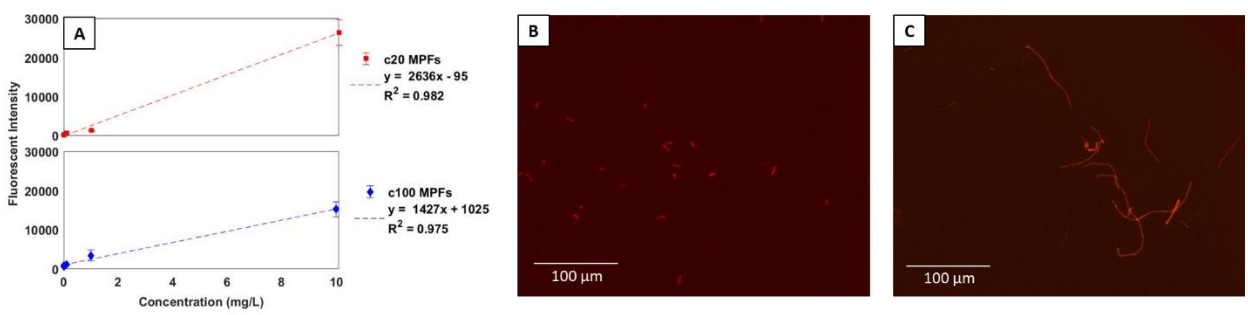

Figure 3.1. Calibration curves (A) of c20 and c100 MPFs using excitation and emission wavelengths of 420 nm and 651 nm respectively. The gain and excitation and emission bandwidth were 190 and 20 nm and 255 and 10 nm for the c20 and c100 MPFs respectively. Fluorescent microscopy images of c20 (B) and c100 MPFs (C).

3.3.2 Effect of Microplastic Fiber Length

Filtration experiments using 5 µm and 0.22 µm PVDF membranes were performed using suspensions of fluorescent MPFs cut at 20 µm and 100 µm, referred to as c20 MPFs and c100 MPFs. Histograms of the length distributions for these MPF samples are shown in Figure 3.4. c20 MPFs had 52% of MPFs between 20 and 30 µm in length and an average length and diameter of of 23 ± 9 µm and 1.3 ± 0.2 µm respectively (where ± is standard deviation). c100 MPFs had a broad length, as noted in the previous chapter, due to the lack of alignment in the electrospun fiber mat as well as potential fragmentation during the cutting process due to the low cryostat temperature. c100 MPFs had an average length of 65 ± 50 µm and 1.1 ± 0.4 µm in diameter. These two MPF samples were compared to understand the difference in MPF transmission and membrane fouling between smaller MPFs and MPFs with a wide length distribution, which are similar to MPF samples from WWTPs [5].

Figure 3.3a and b show average normalized fluorescent intensity measurements for each permeate sample taken during the 4-hour filtration experiments. Normalized fluorescent intensity is reported rather than MPF concentration as MPFs of different sizes may yield different fluorescent intensities. The permeate concentrations of c20 MPFs are significantly higher than the

c100 MPFs for the 5 µm membrane, indicating that the feed suspension consisting of shorter MPFs allowed for increased MPF transmission through the membrane. This is expected as there are more MPFs able to enter the membrane pores of the 5 µm membrane in the c20 MPF sample than in the c100 MPF sample. The amount of MPFs exiting in the permeate is consistent over the 4-hour experiment for both the c20 and c100 MPFs. This is due to the pores of the 5 µm membrane not being completely blocked by MPFs during filtration. As noted in the previous chapter, when MPFs are covering the membrane surface, they are not forming a dense cake layer on top of the membrane. When depositing on the surface, the MPFs are not significantly restricting the membrane pores, allowing a consistent amount of MPFs to pass through. This is confirmed by the permeability and TMP measurements, shown in Figure 3.S4, which were constant for each experiment. If the MPFs were filtered for more than 4 hours, it is expected that the MPFs would eventually cause enough pore blockage to limit MPFs from passing through the membrane.

For the 0.22 µm membrane, the average normalized fluorescence intensity when filtering c20 and c100 MPFs are very similar (standard deviations between 0.0009 and 0.0022) and less than 0.01, indicating minimal transmission through the membrane. The 0.22 µm membrane has pores much smaller than the length and diameter of the MPFs, making it more difficult for MPFs to enter the pores. MPFs would need to be oriented directly into the pore and flow through the tortuous pore structure to make it into the permeate. Operating at higher pressures could facilitate the longitudinal orientation of MPFs with the membrane pores, which could increase their transmission [10]. Since these experiments were operated at low pressure, this is unlikely. A small number of MPFs (11 and 32 MPFs respectively) were observed in the permeate of the 0.22 µm membrane for both the c20 and c100 MPFs, shown in fluorescent microscopy images in Figure 3.3d and f.

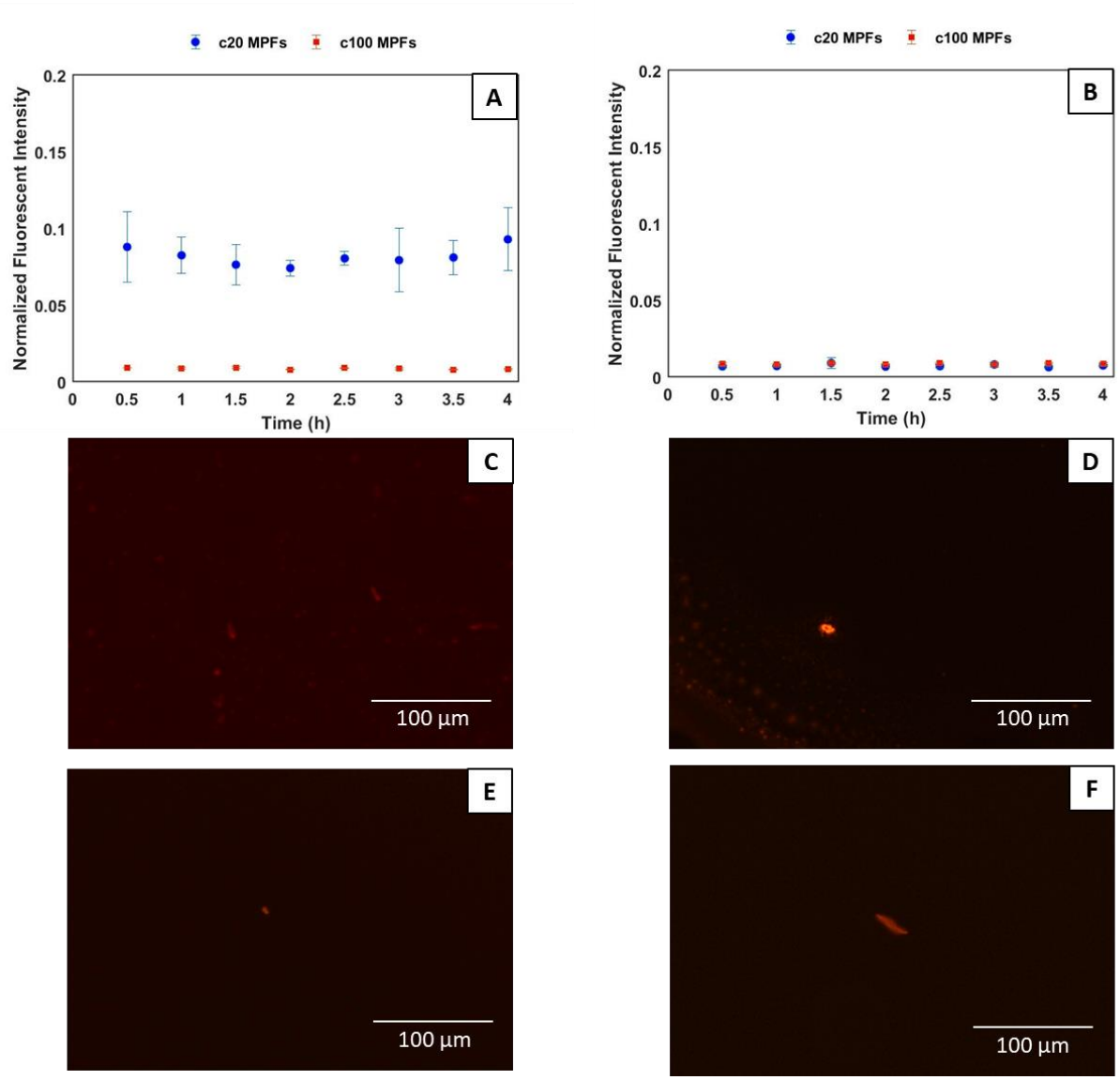

Figure 3.2. Average normalized fluorescent intensity values for permeate samples from filtration experiments using 5 (A) and 0.22 µm (B) membranes with c20 and c100 MPFs. Error bars represent standard deviation. Fluorescent microscopy images of MPFs found in the permeate samples of the 5 µm membrane filtering c20 (C) and c100 (E) MPFs and the 0.22 µm membrane filtering c20 (D) and c100 MPFs (F).

Figure 3.4 shows histograms for the permeate samples from both the 5 µm and 0.22 µm membranes for both c20 and c100 MPFs. For permeate samples from the 5 µm membrane when filtering both MPF samples and the 0.22 µm membrane when filtering c100 MPFs, over 70% of MPFs found in the permeate were less than 10 µm in length. As these are the smallest MPFs, they would have the least resistance to entering the membrane pores as they could enter in different

orientations, especially for the 5 µm membrane where some pores exceed 5 µm. When modelling the rejection of capsular particles by membranes with slit pores, Delavari et al.[30] found that capsular particles with smaller aspect ratios were able to better align with bulk flow, allowing them to more easily pass through the membrane. MPFs less than 10 µm in length would be able to better align with the membrane pores to pass through the membrane compared with longer MPFs. MPFs with lengths much longer than the pore size of the membrane were observed in the permeate samples of the 0.22 µm membrane. As there were very few MPFs observed in these permeate samples, the longer MPFs make up a larger proportion of the total MPFs observed, specifically for the c20 MPFs. To pass through the 0.22 µm membrane, the MPFs would need to pass through the larger pores in the membrane as their length and diameter are significantly larger than the nominal pore size. Since majority of the pore are smaller than the average MPF diameter, few MPFs were able to pass through the membrane. MPs larger than the nominal pore size have been found in the permeate of membrane systems in WWTPs [11].

Understanding the role of MPF size on membrane fouling and MPF rejection is important due to the range of sizes of MPs found in WWTPs. Multiple studies have reported the smallest size fraction measured making up a higher proportion of the permeate compared to the feed during membrane filtration in WWTPs [5][16][17][18]. These findings are important as they indicate that as MPs get smaller, they become more difficult to remove. This is in agreement with the results presented in this work as majority of the MPFs found in the permeate were less than 10 µm, which was the smallest size fraction measured.

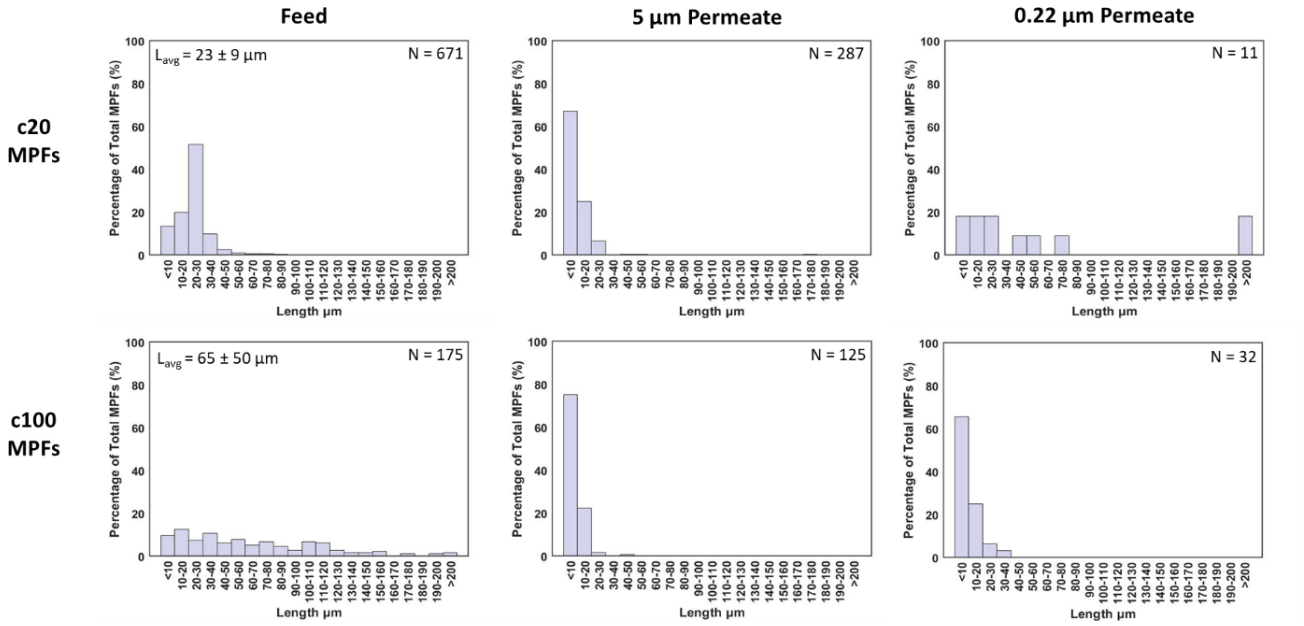

Figure 3.3. Histograms of MPF length in permeate and feed samples for filtration experiments using c20 and c100 MPFs. L_{av} is the average MPF length where ± is the standard deviation. N is the total number of MPFs measured from the feed and permeate in each experiment. The number of MPFs analyzed varies due to the same suspension volume being analyzed for each sample.

Figure 3.5 shows SEM images of both the 5 µm and 0.22 µm membranes after the filtration of c20 and c100 MPFs. The c20 MPFs were observed to be visibly inside the pores of the 5 µm membrane where as the c100 MPFs were seen to be laying on the surface of the membrane or only have a portion of the MPF enter the pores. As permeate results indicate, shorter MPFs are more prone to enter the pores of the 5 µm membrane as they can enter in different orientations and more likely to align with bulk flow [30]. MPFs with lengths greater than the pore size are more limited in how they can enter the pores and are more likely to get trapped on the membrane surface. As the length of both the c20 and c100 MPFs exceed the size of many of the pores in the 0.22 µm membrane, both length distributions of MPFs are observed to be trapped on the membrane surface. This is also consistent with the permeate results as the number of MPFs visually observed in the permeate and the normalized fluorescent intensity of the permeate samples was low for both the c20 and c100 MPFs.

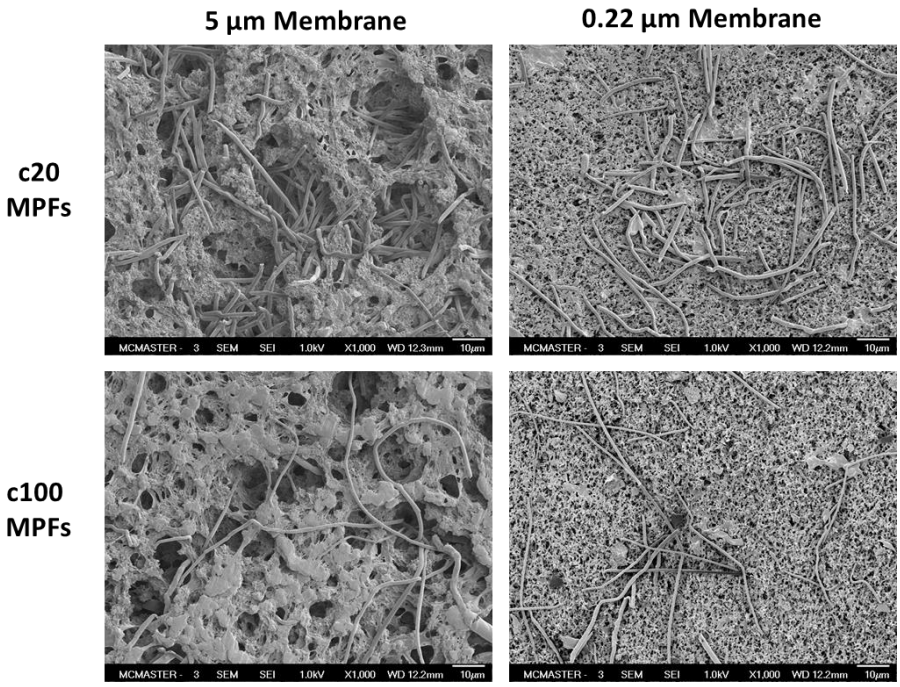

Figure 3.4. SEM images of membrane surface of both 5 µm and 0.22 µm membranes following the filtration of c20 and c100 MPFs.

3.5 Conclusions

In this work, fluorescent MPFs were created by electrospinning a PS solution doped with 2 mg/mL of TPP, enabling their visual detection using fluorescent microscopy as well as detection when suspended in Milli-Q water. The fluorescent MPFs were cut at 20 µm and 100 µm, yielding an aliquot of MPFs with a small average of 23 ± 9 µm (c20 MPFs) and an aliquot of MPFs with an average length of 65 ± 50 µm (c100 MPFs). These two types of fluorescent MPFs were used in filtration experiments with 5 µm and 0.22 µm PVDF membranes, where MPF concentration and length in both the feed and permeate was determined. The c20 MPFs were found to have lower rejection when filtered through the 5 µm membrane compared to the c100 MPFs. The 0.22 µm membrane had nearly complete rejection of both length distributions of MPFs. MPFs less than 10 µm in length were found to be the most prominent in the permeate of the 5 µm membrane for both length distributions, indicating that smaller MPFs are more difficult to remove. Though majority

of the MPFs were rejected by both membranes, showing membrane filtration is effective in MPF removal, the factors impacting MPF transmission such as membrane type, solution conditions, and operating parameters require further research. Creating MPFs that can be easily detected to be used in laboratory experiments allows for different filtration and process conditions to be examined in further detail to understand and prevent the discharge of MPFs into the environment.

3.6 References

[1] D. Eerkes-Medrano, R. C. Thompson, and D. C. Aldridge, "Microplastics in freshwater systems: A review of the emerging threats, identification of knowledge gaps and prioritisation of research needs," *Water Res.*, vol. 75, pp. 63–82, 2015, doi: 10.1016/j.watres.2015.02.012.

[2] V. Hidalgo-Ruz, L. Gutow, R. C. Thompson, and M. Thiel, "Microplastics in the marine environment: A review of the methods used for identification and quantification," *Environ. Sci. Technol.*, vol. 46, no. 6, pp. 3060–3075, 2012, doi: 10.1021/es2031505.

[3] J. Sun, X. Dai, Q. Wang, M. C. M. van Loosdrecht, and B. J. Ni, "Microplastics in wastewater treatment plants: Detection, occurrence and removal," *Water Res.*, vol. 152, pp. 21–37, 2019, doi: 10.1016/j.watres.2018.12.050.

[4] S. M. Mintenig, I. Int-Veen, M. G. J. Löder, S. Primpke, and G. Gerdts, "Identification of microplastic in effluents of waste water treatment plants using focal plane array-based micro-Fourier-transform infrared imaging," *Water Res.*, vol. 108, pp. 365–372, 2017, doi: 10.1016/j.watres.2016.11.015.

[5] J. Talvitie, A. Mikola, A. Koistinen, and O. Setälä, "Solutions to microplastic pollution – Removal of microplastics from wastewater effluent with advanced wastewater treatment technologies," *Water Res.*, vol. 123, pp. 401–407, 2017, doi: 10.1016/j.watres.2017.07.005.

[6] J. Bayo, J. López-Castellanos, and S. Olmos, "Membrane bioreactor and rapid sand filtration for the removal of microplastics in an urban wastewater treatment plant," *Mar. Pollut. Bull.*, vol. 156, no. March, p. 111211, 2020, doi: 10.1016/j.marpolbul.2020.111211.

[7] S. Olmos, J. López-Castellanos, and J. Bayo, "Are advanced wastewater treatment technologies a solution for total removal of microplastics in treated effluents?," *WIT Trans. Ecol. Environ.*, vol. 229, pp. 109–116, 2019, doi: 10.2495/WRM190111.

[8] A. Foglia *et al.*, "Anaerobic membrane bioreactor for urban wastewater valorisation: Operative strategies and fertigation reuse," *Chem. Eng. Trans.*, vol. 74, no. November 2018, pp. 247–252, 2019, doi: 10.3303/CET1974042.

[9] X. Lv, Q. Dong, Z. Zuo, Y. Liu, X. Huang, and W. M. Wu, "Microplastics in a municipal wastewater treatment plant: Fate, dynamic distribution, removal efficiencies, and control

strategies," *J. Clean. Prod.*, vol. 225, pp. 579–586, 2019, doi: 10.1016/j.jclepro.2019.03.321.

[10] H. A. Leslie, S. H. Brandsma, M. J. M. van Velzen, and A. D. Vethaak, "Microplastics en route: Field measurements in the Dutch river delta and Amsterdam canals, wastewater treatment plants, North Sea sediments and biota," *Environ. Int.*, vol. 101, pp. 133–142, 2017, doi: 10.1016/j.envint.2017.01.018.

[11] M. Lares, M. C. Ncibi, M. Sillanpää, and M. Sillanpää, "Occurrence, identification and removal of microplastic particles and fibers in conventional activated sludge process and advanced MBR technology," *Water Res.*, vol. 133, pp. 236–246, 2018, doi: 10.1016/j.watres.2018.01.049.

[12] F. De Falco, E. Di Pace, M. Cocca, and M. Avella, "The contribution of washing processes of synthetic clothes to microplastic pollution," *Sci. Rep.*, no. January, pp. 1–11, 2019, doi: 10.1038/s41598-019-43023-x.

[13] M. Enfrin, J. Lee, P. Le-Clech, and L. F. Dumée, "Kinetic and mechanistic aspects of ultrafiltration membrane fouling by nano- and microplastics," *J. Memb. Sci.*, vol. 601, no. January, 2020, doi: 10.1016/j.memsci.2020.117890.

[14] A. R. P. Pizzichetti, C. Pablos, C. Álvarez-Fernández, K. Reynolds, S. Stanley, and J. Marugán, "Evaluation of membranes performance for microplastic removal in a simple and low-cost filtration system," *Case Stud. Chem. Environ. Eng.*, vol. 3, no. December 2020, p. 100075, 2021, doi: 10.1016/j.cscee.2020.100075.

[15] B. Ma, W. Xue, C. Hu, H. Liu, J. Qu, and L. Li, "Characteristics of microplastic removal via coagulation and ultrafiltration during drinking water treatment," *Chem. Eng. J.*, vol. 359, no. November 2018, pp. 159–167, 2019, doi: 10.1016/j.cej.2018.11.155.

[16] C. Baresel, M. Harding, and J. Fang, "Ultrafiltration/granulated active carbon-biofilter: Efficient removal of a broad range of micropollutants," *Appl. Sci.*, vol. 9, no. 4, 2019, doi: 10.3390/app9040710.

[17] C. Baresel *et al.*, "Membrane Bioreactor Processes to Meet Todays and Future Municipal Sewage Treatment Requirements?," *Int. J. Water Wastewater Treat.*, vol. 3, no. 2, 2017, doi: 10.16966/2381-5299.140.

[18] S. Ziajahromi, P. A. Neale, L. Rintoul, and F. D. L. Leusch, "Wastewater treatment plants as a pathway for microplastics: Development of a new approach to sample wastewater-based microplastics," *Water Res.*, vol. 112, pp. 93–99, 2017, doi: 10.1016/j.watres.2017.01.042.

[19] V. S. Koutnik *et al.*, "Unaccounted Microplastics in Wastewater Sludge: Where Do They Go?," *ACS ES&T Water*, vol. 1, no. 5, pp. 1086–1097, 2021, doi: 10.1021/acsestwater.0c00267.

[20] M. Enfrin, L. F. Dumée, and J. Lee, "Nano/microplastics in water and wastewater treatment processes – Origin, impact and potential solutions," *Water Res.*, vol. 161, pp. 621–638, 2019, doi: 10.1016/j.watres.2019.06.049.

[21] A. Ter Halle *et al.*, “Nanoplastic in the North Atlantic Subtropical Gyre,” *Environ. Sci. Technol.*, vol. 51, no. 23, pp. 13689–13697, 2017, doi: 10.1021/acs.est.7b03667.

[22] M. Hu, W. Kang, Y. Zhao, J. Shi, and B. Cheng, “A fluorescent and colorimetric sensor based on a porphyrin doped polystyrene nanoporous fiber membrane for HCl gas detection,” *RSC Adv.*, vol. 7, no. 43, pp. 26849–26856, 2017, doi: 10.1039/c7ra02040f.

[23] M. Cole, “A novel method for preparing microplastic fibers,” *Sci. Rep.*, vol. 6, no. October, pp. 1–7, 2016, doi: 10.1038/srep34519.

[24] R. Dong, G. Tong, and Y. Zhou, “Self-assembly and optical properties of porphyrin-baed amphiphile,” *Nanoscale*, no. May, 2016.

[25] M. Zhou, H. Liu, J. E. Kilduff, R. Langer, D. G. Anderson, and G. Belfort, “High Throughput Synthesis and Screening of New Protein Resistant Surfaces for Membrane Filtration,” *AIChE J.*, vol. 56, no. 7, pp. 1932–1945, 2010, doi: 10.1002/aic.12104.

[26] A. Senthamizhan *et al.*, “Highly Fluorescent Pyrene-Functional Polystyrene Copolymer Nanofibers for Enhanced Sensing Performance of TNT,” *ACS Appl. Mater. Interfaces*, vol. 7, no. 38, pp. 21038–21046, 2015, doi: 10.1021/acsami.5b07184.

[27] K. R. Stoll, F. Scholle, J. Zhu, X. Zhang, and R. A. Ghiladi, “BODIPY-embedded electrospun materials in antimicrobial photodynamic inactivation,” *Photochem. Photobiol. Sci.*, vol. 18, no. 8, pp. 1923–1932, 2019, doi: 10.1039/c9pp00103d.

[28] L. Huang *et al.*, “Electrospinning preparation and optical transition properties of Eu(DBM) 3Phen/PS fluorescent composite fibers,” *Opt. Commun.*, vol. 285, no. 6, pp. 1476–1480, 2012, doi: 10.1016/j.optcom.2011.10.006.

[29] P. Rothemund, “A new porphyrin synthesis. THe synthesis of porphin,” *J. Am. Chem. Soc*, vol. 157, no. 6, pp. 625–627, 1936.

[30] A. Delavari, B. Agasanapura, and R. E. Baltus, “The effect of particle rotation on the motion and rejection of capsular particles in slit pores,” *AIChE J.*, vol. 64, no. 7, pp. 2828–2836, 2018, doi: 10.1002/aic.16132.

3.7 Supplemental Information

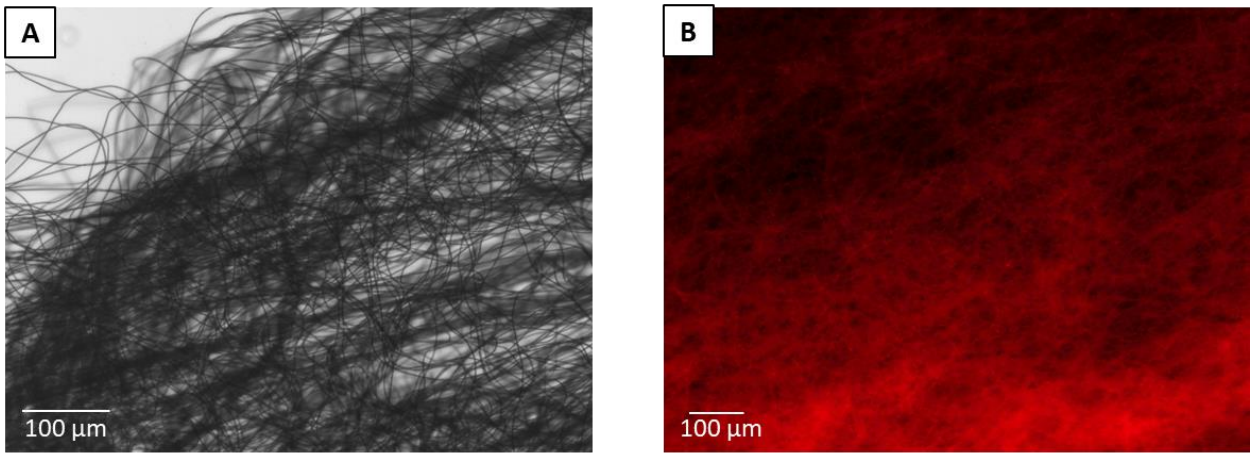

Figure 3.S1. Brightfield (A) and fluorescent (B) images of electrospun fiber mats of PS fibers doped with TPP.

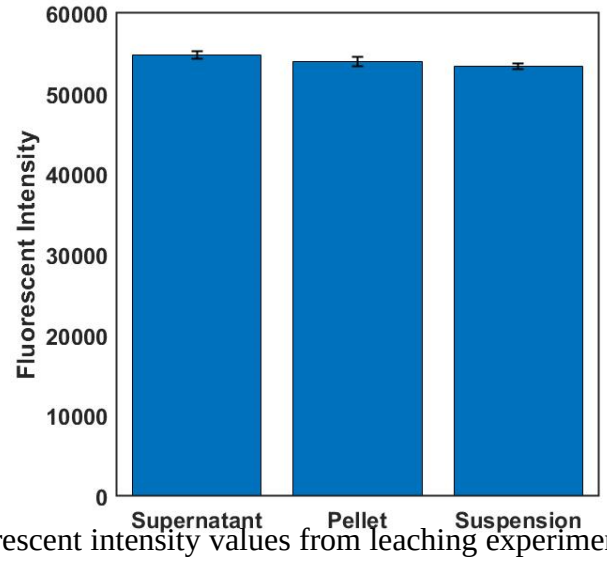

Figure 3.S2. Fluorescent intensity values from leaching experiment using MPFs doped with 0.17 w/v% fluorescein. MPFs suspended in Milli-Q water were centrifuged at 10000 rpm for 1 hour. The supernatant, which was visibly free of MPFs, was removed after centrifuging. 150 µL of the supernatant, pellet, and original suspension were put in a black half area 96-well plate and the fluorescent intensity was measured using a plate reader using excitation and emission wavelengths of 485 nm and 535 nm respectively. All three samples had similar fluorescent intensities, indicating fluorescein had leached from the MPFs.

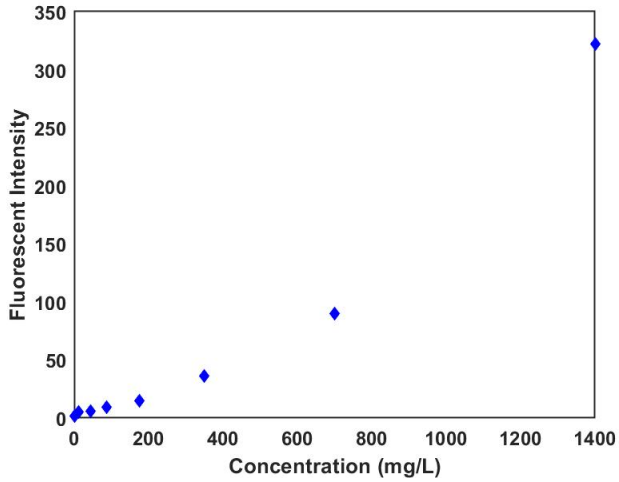

Figure 3.S3. Fluorescent intensity values for concentrations of 0 – 1400 mg/L of MPFs doped with 0.25 w/v% anthracene. Fluorescent intensity was measured at excitation and emission wavelengths of 360 nm and 400 nm respectively.

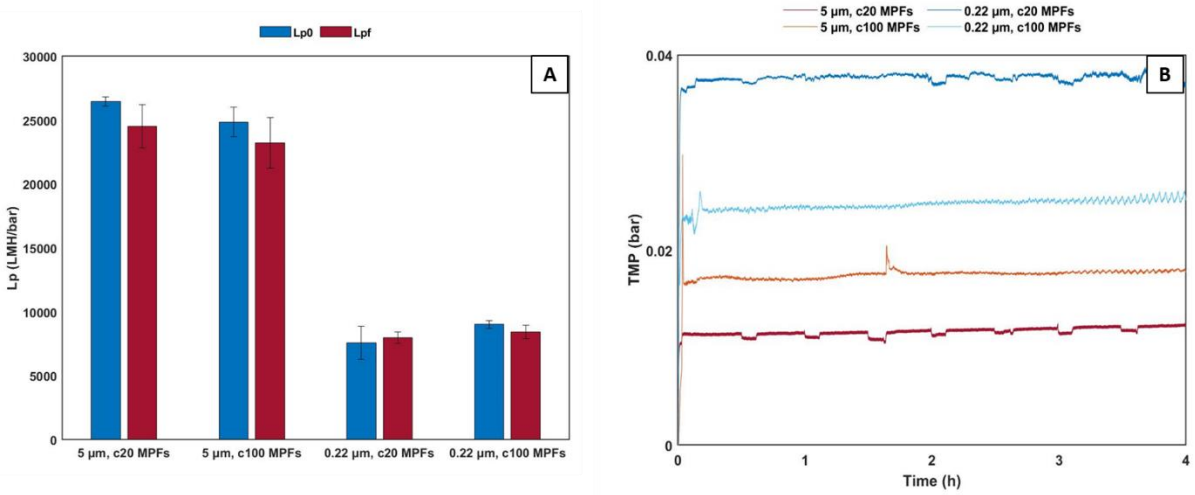

Figure 3.S4. Average permeability values (A) and TMP profiles (B) for filtration experiments using c20 and c100 MPFs with both 5 µm and 0.22 µm membranes.

Chapter 4: Conclusions and Future Work

4.1 Conclusions

Polystyrene MPFs were fabricated by combining polymer electrospinning with a cryostat cutting process. The MPFs produced were found to be suitable model particles for MPFs found in WWTPs as they were of similar lengths to those found in WWTPs and made of a polymer chemistry commonly found among MP samples. Two different length distributions were created by cutting the electrospun fibers at different length settings on the cryostat, enabling the investigation of how MPF properties impact membrane filtration. Fluorescent MPFs were created by doping the electrospinning solution with TPP, allowing for MPFs to be detected visually using fluorescent microscopy and in suspension by measuring fluorescent intensity.

Non-fluorescent MPFs averaging 73 ± 48 μm in length and 0.52 ± 0.08 μm in diameter were used in filtration experiments investigating the effect of MPF concentration, membrane pore size, and solution conditions. When suspended in Milli-Q water, MPFs at concentrations ranging from 5 - 100 mg/L were found to not significantly contribute to membrane fouling when filtered through a 0.22 μm PVDF membrane. MPFs were found to lay on the surface of the membrane, forming a loose cake layer at the higher concentrations tested due to their irregular stacking. MPFs were found to permeate through a 5 μm membrane, with the MPFs found in the permeate being significantly smaller than the average length of MPFs in the feed. MPFs larger than 5 μm were found in the permeate as many of the membrane pores are larger that 5 μm. Suspending the MPFs in WW from a municipal WWTP increased the fouling effects for the both 0.22 μm and 5 μm membranes, showing the importance of realistic solution conditions in understanding MPF filtration.

Fluorescent MPFs were used to further investigate the transmission of MPFs through 5 µm and 0.22 µm PVDF membranes. Fluorescent MPFs were cut at two different lengths 20 µm and 100 µm to yield MPFs averaging 23 ± 9 µm (c20 MPFs) and 65 ± 50 µm (c100 MPFs) respectively. When filtered through the 5 µm membrane, the c20 MPFs produced more MPFs in the permeate than the c100 MPFs when detected using fluorescent intensity measurements. The 0.22 µm membrane had nearly complete rejection of both c20 and c100 MPFs, though MPFs were still detected in the permeate using fluorescent microscopy. MPFs less than 10 µm in length were found to be the most prominent in the permeate, showing that smaller MPFs are more difficult to remove, even when they are larger than the nominal membrane pore size.

This work demonstrates the impact of MPFs on membrane filtration by investigating MPF, membrane, and solution properties. A key finding was the need to conduct experiments under conditions realistic to those in WWTPs. Here we have created MPFs that are of relevant size and chemistry, used membranes of common materials and pore sizes, and used real WW to better understand the filtration of MPFs. The creation of fluorescent MPFs has improved MPF detection in laboratory experiments, further developing the understanding of MPF transmission through membranes. This work is the first of its kind as all works currently published on the filtration of MPs at the laboratory scale have focused on MP fragments/particles. This work is therefore a stepping stone to better understanding MPF removal using membranes and how to prevent their discharge into the environment.

4.2 Future Work

A natural continuation of this work would be the investigation of spatial deposition of MPFs within the membrane. Creating fluorescent MPFs would allow for them to be viewed within the

membrane using confocal microscopy. This would provide more insight into how MPFs are being transmitted through the membrane, particularly for the 5 µm membrane, where a significant number of MPFs were found in the permeate. Filtration studies investigating virus purification using fluorescent nanoparticles [1] and fluorescent bacteriophage [2] have used confocal microscopy to understand particle capture and penetration within membranes. Confocal microscopy has also been used to investigate the impacts of uptake of MPs within plants [3]. Using confocal microscopy would allow for better understanding of how MPFs are penetrating into the membrane and where they are captured within it. The impact of different MPF properties could also be investigated by creating MPFs with different properties such as diameter, length, or chemistry and using different fluorophores for MPFs with these different properties. This would enable to comparison of MPFs in the permeate using fluorescence measurements or within the membrane itself using confocal microscopy.

Though PS is a common polymer chemistry found in MP samples from WWTPs, it is not commonly found in MPFs specifically. As a common source of MPFs is the laundering of synthetic textiles, the MPF fabrication technique used in this work could be used with polymers that are commonly used for synthetic textiles such as nylon, polyethylene terephthalate, and polypropylene. Nylon [4], polyethylene terephthalate [5], and polypropylene [6] have documented electrospinning processes which could be combined with cryostat cutting to generate more realistic MPFs. Working with MPFs made of polymers more commonly found in samples of MPFs from WWTPs would allow for a more detailed understanding of the interactions between MPFs and the membrane surface.

The impact of MPF size could be further investigated by creating MPFs with longer lengths and more narrow length distributions than those studied in Chapter 3. Improving fiber alignment

when electrospinning would cause less variation in length when cutting the fiber mat using the cryostat. Fiber alignment could be improved by increasing the rotation speed of the rotating drum collector [7] or changing the collector to one that is better suited to aligned fibers. Teo and Ramakrishna [8] used two steel blades with a gap in between them which acted as counter electrodes to collect electrospun fibers in highly ordered fiber bundles. Nguyen et al [9] achieved highly aligned fibers by fitting a rotating drum collector with two curved dielectric films which intensified the electrostatic field in a desired area. The cryostat used in this study has a maximum cut length of 300 µm, which could allow for better comparison between MPF lengths. Narrow length distributions could also be achieved by separating MPFs by length following the cryostat cutting process. Differential centrifugation has been used to separate different sizes of spherical particles [10] and has been applied to separate different lengths of gold nanorods [11]. To chose the appropriate centrifugation speeds and settling time for the MPFs, the drag coefficient for non-spherical particles proposed by Hölzer and Sommerfeld [12] could be used. As well, the electrospinning process allows the user to change the diameter of the fibers by modifying electrospinning parameters such as collector to needle distance, solution feed rate, and applied voltage [13]. Polystyrene can be electrospun into fibers 0.3 – 4.3 µm in diameter [14]. Investigating MPF diameter as well as length will allow for a better understanding of the effects of MPF size on membrane filtration and MPF rejection.

In this study, dead-end filtration experiments using flat sheet membranes were performed as this was an initial investigation into the filtration of MPFs. To better understand the filtration of MPFs in systems realistic to those used in WWTPs, membrane configurations and operating conditions found in WWTPs should be used. Initial experiments could use individual hollow fiber (HF) or flat sheet membranes operated in cross-flow to better understand how this operating format

and different membrane geometries impact MPF filtration. This would involve working with UF HF membranes such as the ZeeWeed membranes from Suez, which have a 0.04 µm pore size [15]. These processes could then be scaled to use HF or spiral wound membrane modules and eventually move to pilot scale experiments where MPF filtration over time could be investigated. Using the MPF fabrication method presented in this work, enough MPFs could be produced to run pilot scale experiments by extending the electrospinning time to 8 hours, using approximately 1 mL of polymer solution. This would produce enough MPFs to run experiments using a concentration of 1 mg/L of MPFs using a pilot scale membrane system with a working volume of 3.2 m^3 [16]. Though this work gives insight into the filtration of MPFs, it is only a first step in understanding how MPFs interact with membranes and how their transmission can be prevented.

4.3 References

[1] F. Fallahianbijan, S. Giglia, C. Carbrello, and A. L. Zydney, "Use of fluorescently-labeled nanoparticles to study pore morphology and virus capture in virus filtration membranes," *J. Memb. Sci.*, vol. 536, no. February, pp. 52–58, 2017, doi: 10.1016/j.memsci.2017.04.066.

[2] M. Bakhshayeshi, N. Jackson, R. Kuriyel, A. Mehta, R. van Reis, and A. L. Zydney, "Use of confocal scanning laser microscopy to study virus retention during virus filtration," *J. Memb. Sci.*, vol. 379, no. 1–2, pp. 260–267, 2011, doi: 10.1016/j.memsci.2011.05.069.

[3] T. Bosker, L. J. Bouwman, N. R. Brun, P. Behrens, and M. G. Vijver, "Microplastics accumulate on pores in seed capsule and delay germination and root growth of the terrestrial vascular plant Lepidium sativum," *Chemosphere*, vol. 226, pp. 774–781, 2019, doi: 10.1016/j.chemosphere.2019.03.163.

[4] H. Fong, W. Liu, C. S. Wang, and R. A. Vaia, "Generation of electrospun fibers of nylon 6 and nylon 6-montmorillonite nanocomposite," *Polymer (Guildf).*, vol. 43, no. 3, pp. 775–780, 2001, doi: 10.1016/S0032-3861(01)00665-6.

[5] Z. Ma, M. Kotaki, T. Yong, W. He, and S. Ramakrishna, "Surface engineering of electrospun polyethylene terephthalate (PET) nanofibers towards development of a new material for blood vessel engineering," *Biomaterials*, vol. 26, no. 15, pp. 2527–2536, 2005, doi: 10.1016/j.biomaterials.2004.07.026.

[6] K. H. Lee *et al.*, “Electrospinning of syndiotactic polypropylene from a polymer solution at ambient temperatures,” *Macromolecules*, vol. 42, no. 14, pp. 5215–5218, 2009, doi: 10.1021/ma9006472.

[7] E. Saino *et al.*, “Effect of electrospun fiber diameter and alignment on macrophage activation and secretion of proinflammatory cytokines and chemokines,” *Biomacromolecules*, vol. 12, no. 5, pp. 1900–1911, 2011, doi: 10.1021/bm200248h.

[8] W. E. Teo and S. Ramakrishna, “Electrospun fibre bundle made of aligned nanofibres over two fixed points,” *Nanotechnology*, vol. 16, no. 9, pp. 1878–1884, 2005, doi: 10.1088/0957-4484/16/9/077.

[9] D. N. Nguyen, Y. Hwang, and W. Moon, “Electrospinning of well-aligned fiber bundles using an End-point Control Assembly method,” *Eur. Polym. J.*, vol. 77, pp. 54–64, 2016, doi: 10.1016/j.eurpolymj.2016.02.017.

[10] J. D. Robertson *et al.*, “Purification of Nanoparticles by Size and Shape,” *Sci. Rep.*, vol. 6, pp. 1–9, 2016, doi: 10.1038/srep27494.

[11] R. Wang, Y. Ji, X. Wu, R. Liu, L. Chen, and G. Ge, “Experimental determination and analysis of gold nanorod settlement by differential centrifugal sedimentation,” *RSC Adv.*, vol. 6, no. 49, pp. 43496–43500, 2016, doi: 10.1039/c6ra07829j.

[12] A. Hölzer and M. Sommerfeld, “New simple correlation formula for the drag coefficient of non-spherical particles,” *Powder Technol.*, vol. 184, no. 3, pp. 361–365, 2008, doi: 10.1016/j.powtec.2007.08.021.

[13] A. Greiner and J. H. Wendorff, “Electrospinning: A fascinating method for the preparation of ultrathin fibers,” *Angew. Chemie - Int. Ed.*, vol. 46, no. 30, pp. 5670–5703, 2007, doi: 10.1002/anie.200604646.

[14] T. Uyar and F. Besenbacher, “Electrospinning of uniform polystyrene fibers : The effect of solvent conductivity,” *Polymer (Guildf).*, vol. 49, no. 24, pp. 5336–5343, 2008, doi: 10.1016/j.polymer.2008.09.025.

[15] S. W. T. & Solutions, “ZeeWeed 500 Membrane,” 2021. https://www.suezwatertechnologies.com/products/ultrafiltration/zeeweed-500-membrane (accessed Aug. 09, 2021).

[16] N. Ren, Z. Chen, X. Wang, D. Hu, and A. Wang, “Optimized operational parameters of a pilot scale membrane bioreactor for high-strength organic wastewater treatment,” *Int. Biodeterior. Biodegrad.*, vol. 56, no. 4, pp. 216–223, 2005, doi: 10.1016/j.ibiod.2005.08.003.

Appendix A

A.1 Microplastic Fiber Synthesis Protocol

A.1.1 Electrospinning

To create the electrospinning solution, polystyrene (PS, M_w ~192000 g/mol) is added to N,N,dimethylformamide (DMF) to create a 30 wt% polymer solution. To create fluorescent MPFs, meso - tetraphenylporphyrin (TPP) is added at a concentration of 2 mg/mL. The polymer solution is vortexed several times then mixed overnight using a magnetic stir bar and stir plate. Fluorescent electrospinning solutions are kept in the dark to prevent photobleaching. Once the PS and TPP is dissolved, the solution is loaded into a 1 mL syringe with a 25-gauge blunt needle. The syringe filled with polymer solution is loaded onto a syringe pump which is used to extrude the solution at a rate of 2 µL/min. A voltage of 15 kV is applied to the tip of the needle using a high voltage power supply to electrospin the PS solution. The electrospun fibers are collected using a rotating drum collector 3 cm in diameter, rotating at a speed of 2000 rpm. Aluminum foil is wrapped tightly around the rotating drum collector to allow the electrospun fiber mat to be easily removed when finished electrospinning. The distance between the needle and collector was varied between 5 – 10 cm. The electrospinning equipment was used inside of a fumehood as the DMF will evaporate as the fiber mat is created. Adjusting the parameters in the electrospinning process can change the morphology of the fibers. For instance, increasing the applied voltage, increasing polymer feed rate, decreasing solution conductivity, increasing polymer concentration, and decreasing the distance between the needle tip and collector have been found to increase fiber diameter [1][2]. Figure A.1 shows a picture of the electrospinning set up. The PS solution can be electrospun for any length of time desired (a greater solution volume and larger syringe would be required for longer times) based on the amount of MPFs required for experiments. To determine alignment, morphology, and fluorescence of the fiber mat, PS solution was electrospun for 5 – 10 minutes

and transferred from the aluminum foil to a glass slide and covered with a coverslip to be viewed using optical microscopy. Fiber mats intended to be cut into MPFs were electrospun for 0.5 – 2 hours. When the aluminum foil with the electrospun mat was removed from the collector, it was gently laid flat and stored in a plastic bag prior to freezing and cutting.

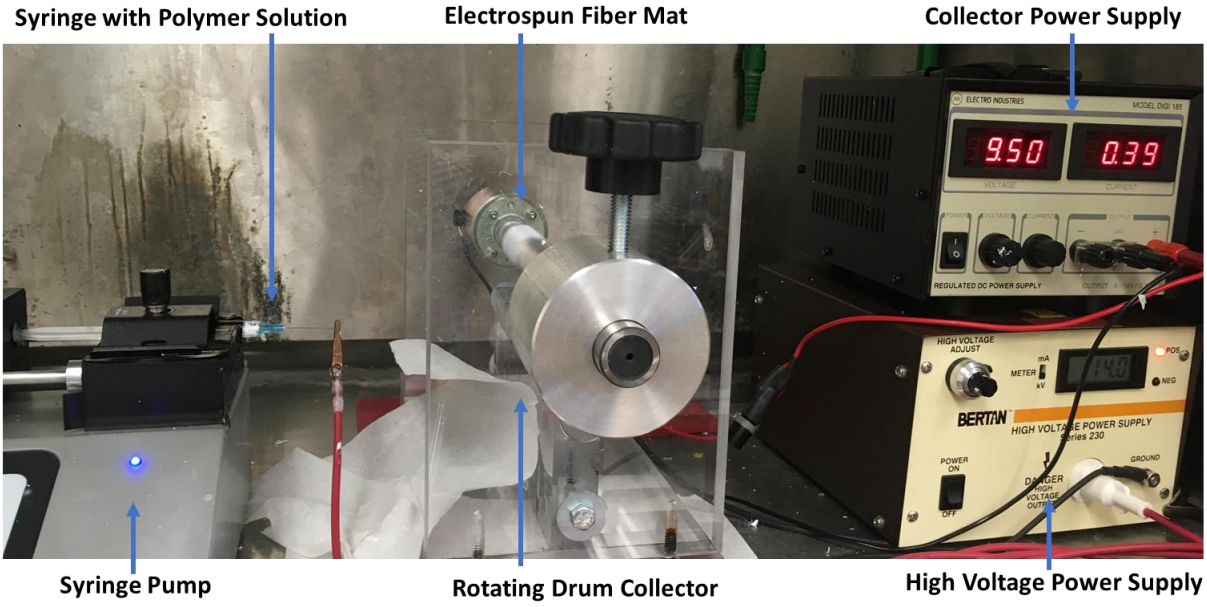

Figure A.1. Electrospinning set-up.

A.1.2 Freezing and Cutting

Before cryostat cutting, the electrospun fiber mat on aluminium foil was coated in freezing compound (Tissue-Tek) and placed in a -20^{o}C freezer for at least twenty minutes or until the freezing compound is completely white and opaque. Once the coated fiber mat is frozen, it can be cut into sections to be able to fit onto the cryostat chuck. This is done by cutting the frozen fiber mat in half using a razor blade and stacking one half on top of the other with freezing compound placed in between and freezing for at least 20 minutes. This process is repeated until the fiber mat is frozen into a block approximately 1.5 cm in length, width, and height maximum, with smaller

blocks able to fit better on the cryostat chuck. The frozen block should be as uniform as possible and any protruding edges removed prior to cutting. Images of the electrospun mat and frozen mat are shown in Figure A.2.

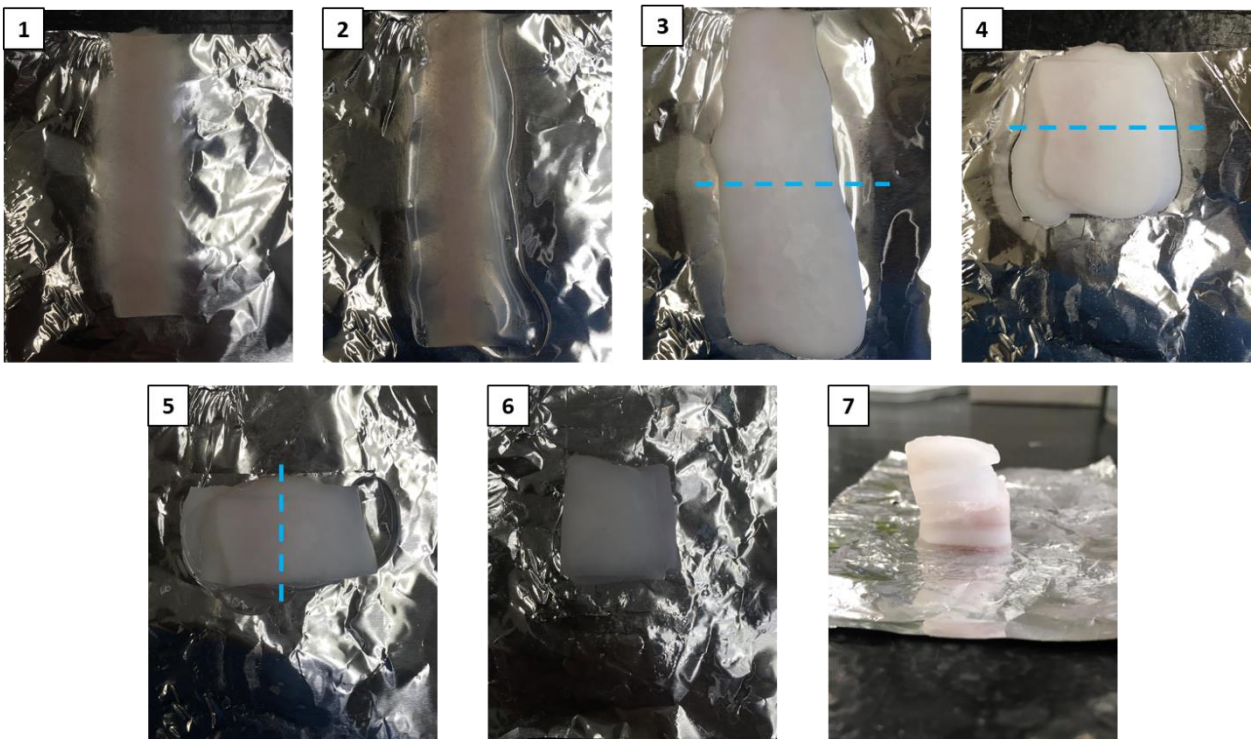

Figure A.2. Example of frozen and cut cryostat mat. The electrospun mat (1) is covered in the freezing compound (2) and frozen in a -20°C freezer for at least 20 minutes. Once the mat is completely frozen (3) it is cut in half and the halves are stuck together using the freezing compound (4). This is repeated until the mat is small enough to fit onto the cryostat chuck (5-7).

Once the frozen block is prepared it is ready for cryostat cutting. The block is mounted on the cryostat chuck using freezing compound, ensuring the block is oriented so that the frozen layers are vertical to prevent the block coming apart during cutting. Figure A.3 shows a diagram of how the fiber mat is oriented on the cryostat chuck. The block is first trimmed on the cryostat at a trim setting of 150 µm until a flat surface on the block is achieved. The block can then be cut into MPFs

at cut settings between 0.5 - 300 µm (based on the Leica CM3050 cryostat settings). During cutting the anti-roll guard is placed over the cutting surface to collect MPFs. To maintain consistent cuts, the anti-roll guard is left in place during the entire cut, with MPFs being removed only around the edges of the cut surface until finished cutting the entire block. The frozen MPFs are placed into a glass vial using tweezers. Figure A.4 shows an image of the cryostat while cutting MPFs.

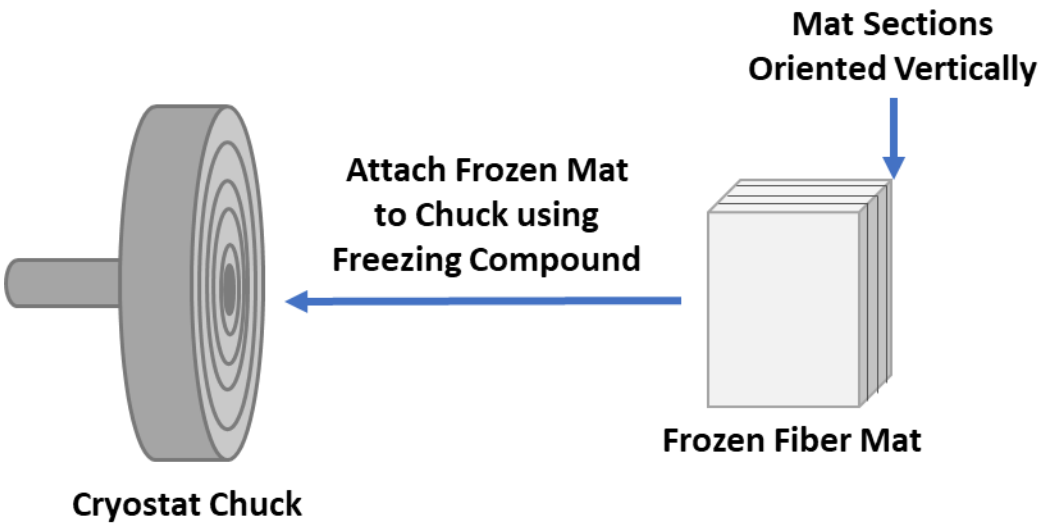

Figure A.3. Diagram of frozen fiber mat placement on cryostat chuck.

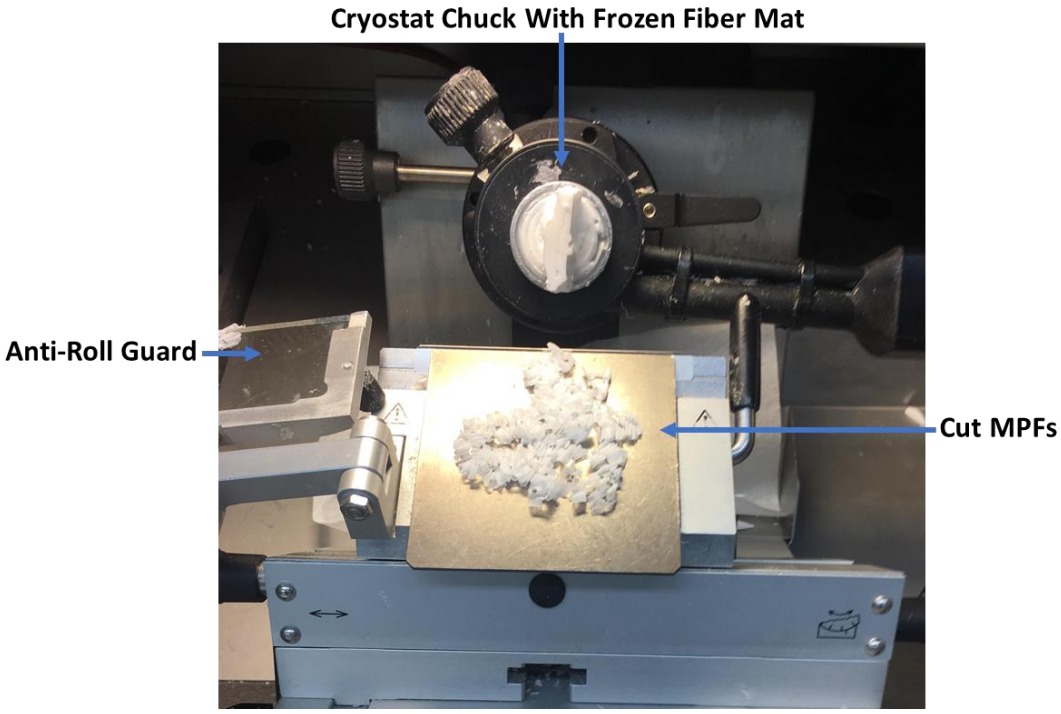

Figure A.4. Cryostat cutting of a frozen electrospun fiber mat into MPFs.

A.1.3 Post-Cutting and Purification

Once the MPFs are cut, the glass vial is filled with Milli-Q water and vortexed to distribute the MPFs. The suspended MPFs are mixed overnight using a magnetic stir bar and stir plate. Following mixing, the freezing compound can be removed by passing several milliliters of suspended MPFs through a qualitative filter paper that is placed in a Cole-Parmer filter holder using a syringe. After passing the MPF solution through the filter paper, the syringe can be filled with air which is passed through the filter paper to removed as much water as possible. The MPFs retained by the filter paper can be gently scrapped off using tweezers and weighed to determine their mass. The purified MPFs are placed in a centrifuge tube filled with 1 mL of Milli-Q water. The centrifuge tube is then sonicated for 30 minutes to disaggregate the MPFs. This stock solution of MPFs can then be diluted for use in filtration experiments. Fluorescent MPFs are stored in the dark to prevent photobleaching.

A.2 References

[1] A. Haider, S. Haider, and I. K. Kang, “A comprehensive review summarizing the effect of electrospinning parameters and potential applications of nanofibers in biomedical and biotechnology,” *Arab. J. Chem.*, vol. 11, no. 8, pp. 1165–1188, 2018, doi: 10.1016/j.arabjc.2015.11.015.

[2] A. Greiner and J. H. Wendorff, “Electrospinning: A fascinating method for the preparation of ultrathin fibers,” *Angew. Chemie - Int. Ed.*, vol. 46, no. 30, pp. 5670–5703, 2007, doi: 10.1002/anie.200604646.